Proximal braided-river morphodynamics reconstructed through ground-penetrating radar and multi-temporal remote sensing: Kicking Horse River, British Columbia, Canada

by

Natasha Nicole Cyples

A thesis submitted in partial fulfillment
of the requirements for the degree of
Master of Science (MSc) in Geology

The Faculty of Graduate Studies
Laurentian University
Sudbury, Ontario, Canada

THESIS DEFENCE COMMITTEE/COMITÉ DE SOUTENANCE DE THÈSE
Laurentian Université/Université Laurentienne
Faculty of Graduate Studies/Faculté des études supérieures

Title of Thesis Titre de la thèse	Proximal braided-river morphodynamics reconstructed through ground-penetrating radar and multi-temporal remote sensing: Kicking Horse River, British Columbia, Canada
Name of Candidate Nom du candidat	Cyples, Natasha
Degree Diplôme	Master of Science
Department/Program Département/Programme	Geology
Date of Defence Date de la soutenance	December 07, 2018

APPROVED/APPROUVÉ

Thesis Examiners/Examinateurs de thèse:

Dr. Alessandro Ielpi
(Co-Supervisor/Co-directeur de thèse)

Dr. Randy Dirszowsky
(Co-Supervisor/Co-directeur de thèse)

Dr. Richard Smith
(Committee member/Membre du comité)

Dr. Stephen Hubbard
(External Examiner/Examinateur externe)

Approved for the Faculty of Graduate Studies
Approuvé pour la Faculté des études supérieures
Dr. David Lesbarrères
Monsieur David Lesbarrères
Dean, Faculty of Graduate Studies
Doyen, Faculté des études supérieures

ACCESSIBILITY CLAUSE AND PERMISSION TO USE

Abstract

Located in southeastern British Columbia, the Kicking Horse River is a gravel-bed braided river that flows westward through the Canadian Rocky Mountains. Prior studies focused on using ground observations to describe processes of bar formation and sediment distribution patterns; however, a complete model of planform evolution and related stratigraphic signature is lacking. The river was re-examined combining ground observations, multi-temporal remote sensing, discharge data, and ground-penetrating radar to develop three-dimensional models of bar geometry and to highlight changes in alluvial morphology. Remote sensing indicates extensive lateral channel migration over an eight-year period and demonstrates how varying flood stages are associated with episodes of channel braiding. Ground-penetrating radar imaging and analysis identified the distribution of sedimentary facies in the subsurface, which were used to understand the river's depositional history. The Kicking Horse River's sedimentary signature is compared to those of both proximal, coarse-grained and more distal, mixed sandy-gravel fluvial systems where similarities in sedimentary architecture and fluvial processes are observed.

Keywords

Braided, fluvial, British Columbia, sedimentology, remote sensing, ground-penetrating radar

Co-Authorship Statement

Chapter 2 is written as a journal manuscript co-authored by N. N. Cyples, A. Ielpi, and R.W. Dirszowsky. Field work was completed by the candidate in August 2016 and October 2016 under the supervision of Dr. Ielpi and Dr. Dirszowsky. Ground-penetrating radar (GPR) data was processed and corrected by Dr. Dirszowsky. The first draft and initial interpretations were completed by the candidate with guidance from Dr. Ielpi. The co-authors edited subsequent drafts of the manuscript and provided scientific input for the candidate to investigate and follow up on.

Acknowledgements

I would like to express my sincere gratitude to my supervisor, Dr. Alessandro Ielpi for providing me with this amazing opportunity and making my M.Sc. experience absolutely incredible. Thank you for your constant guidance, expertise, patience, and friendship throughout the study. Thank you to my co-supervisor, Dr. Randy Dirszowsky for your encouragement and insightful comments along the way.

I would like to thank my fellow lab mates who have become some of my best friends: Lorraine Lebeau, Robbie Meek, and Sophie Michel for their constant support and knowledge; I could not have done this without you! Last but not least, a wholehearted thank you to Keaton Strongman for putting up with me through this entire process and for always pushing me to do my best! This project was financially supported by Laurentian University and a Discovery Grant from the Natural Sciences and Engineering Research Council of Canada.

Table of Contents

List of Figures

List of Appendices

Chapter 1

1. Introduction to thesis

1.1 Statement of the problem

This thesis investigates the sedimentology, remote sensing, discharge records, and ground-penetrating radar (GPR) of the Kicking Horse River in Field, British Columbia, a mountainous river that can be used as a facies model for proximal, braided-fluvial sedimentation. A 7-km-long reach of the Kicking Horse River was examined near the town of Field, British Columbia; there, an active alluvial plain is situated between the Trans-Canada Highway and the Canadian Pacific Railway. Planform observations of the river were originally described by Smith (1974) who identified processes of bar formation and sediment distribution patters solely from ground observations. Another study conducted by Hein and Walker (1977) elaborated on the sedimentology, focusing on the hydraulic parameters of the river. The planform of the Kicking Horse River is further investigated in this thesis, while integrating other analyses such as remote sensing and ground-penetrating radar to understand the river's depositional history. Ground-penetrating radar has been increasingly used on a number of well-developed braided river systems where the sedimentology has been well documented, producing high-resolution 2-D and 3-D depositional models. These studies are however biased towards systems occupying distal alluvial plains, leaving a gap in knowledge for more proximally located (i.e. close to the river's glacial source) fluvial systems such as the Kicking Horse River. This study seeks to fill that gap by linking patterns of morphodynamic change in

planform to detailed three-dimensional subsurface profiles, in order to create a more refined depositional model of the Kicking Horse River.

1.2 Goals and research questions

- To advance the general understanding of the dominant fluvial processes and architectural elements governing the evolution of the Kicking Horse River both in planform and in the subsurface.

The Kicking Horse River is a gravel-bed braided river that has been recognized as a facies model for braided river deposition. The sedimentology of the river was studied in the 1970's (Smith 1974; Hein and Walker 1977), but a sophisticated depositional model is lacking. Sedimentology in addition to remote sensing and ground-penetrating radar imaging can be integrated to create a depositional model of the river, and to understand planform dynamics and the key depositional processes governing the river.

- To understand the depositional history of the Kicking Horse River in terms of radar facies and depositional processes inferred from ground-penetrating radar data.

Numerous studies have been published using ground-penetrating radar to examine alluvial architecture in braided rivers and yielded interesting results. To develop a complete facies model of the Kicking Horse River requires extensive analysis of not only the planform sedimentology, but also the subsurface architecture. Ground-penetrating radar allows depiction of the architectural elements that are preserved, offering a foundation for comparisons with the depositional record of other fluvial systems.

- To develop a three-dimensional model displaying the architectural elements that are preserved, and their relative abundance in upstream versus downstream reaches of the alluvial plain.

Discerning sedimentary structures in the subsurface and relating them to specific architectural elements and fluvial processes allows for the creation of a high-resolution three-dimensional facies model of the subsurface. The quantitative analysis and relative abundances of preserved architectural elements may shed light on the depositional history of the river in different portions of its alluvial plain. These observations can be compared and combined with observations from other rivers, to develop more comprehensive and inclusive facies model of braided-fluvial deposition.

- Can the Kicking Horse River be related to river types other than proximal gravel-bed rivers?

The Kicking Horse River is a rather unique example, in that it is proximally-sourced by glaciers, but exhibits depositional processes of both gravel-bed rivers and more distal-sandier systems. The comparison with transitional, gravel-/sand-bed rivers may highlight similarities with a broader spectrum of modern fluvial morphodynamics.

1.3 Structure of thesis

The thesis is presented in three chapters. Chapter 2 is written as a manuscript for publication in a refereed scientific journal. The manuscript will be published as an independent article, so there is repetition in the introduction of each chapter. Chapter 2 is entitled "**Proximal braided-river morphodynamics reconstructed through ground-penetrating radar and multi-temporal remote sensing: Kicking Horse River, British**

Columbia, Canada", and is to be submitted to *The Journal of Sedimentary Research*. This paper links planform and subsurface sedimentology using multi-temporal remote sensing in conjunction with discharge records and GPR and presents a three-dimensional depositional model of the river.

1.4 Statement of responsibilities

Field work was completed by the candidate with the assistance and supervision of Dr. Alessandro Ielpi and Dr. Randy Dirszowsky. Field work was completed in August 2016 and October 2016. Dr. Dirszowsky was invited as a co-author and secondary supervisor for his expertise on geomorphology and the use of ground-penetrating radar equipment. The initial draft and interpretation of Chapter 2 were written by the candidate with editing by Dr. Ielpi and Dr. Dirszowsky.

1.5 Statement of original contributions

The following points outline the original contributions made by this study:

- Re-examines the different aspects of sedimentology of the Kicking Horse River and provides a revised interpretation of the channel types and barforms dominant in planform.
- Documents paleoflow measurements, degree of vegetation cover, and flow divergence values measured for ten braid bars.
- Infers/describes history of braid-bar growth and dissection and their morphological evolution.
- Provides estimates of rates of lateral migration derived from satellite imagery over an eight-year period.

- Integrates planform observations with remote sensing and ground-penetrating radar for the first time in the study area, in order to develop a three-dimensional depositional model.

1.6 References

Hein, F.J., and Walker, R.G., 1977, Bar evolution and development of stratification in the gravelly, braided, Kicking Horse River, British Columbia: Canadian Journal of Earth Sciences, v. 14, p. 562-570.

Smith, N.D., 1974, Sedimentology and bar formation in the Upper Kicking Horse River, a braided outwash stream: The Journal of Geology, v. 82, p. 205-223.

Chapter 2

2. Proximal braided-river morphodynamics reconstructed through ground-penetrating radar and multi-temporal remote sensing: Kicking Horse River, British Columbia, Canada

Natasha N. Cyples*[1], Alessandro Ielpi[1] and, Randy W. Dirszowsky[2]

[1]Harquail School of Earth Sciences, Laurentian University, Sudbury, Ontario P3E 2C6, Canada. [2]School of the Environment, Laurentian University, Sudbury, Ontario P3E 2C6, Canada.

* Corresponding author at: Harquail School of Earth Sciences, Laurentian University, 935 Ramsey Lake Road, Sudbury, ON, Canada P3E 2C6. Tel./fax: +1 705 675 1151.

E-mail address: ncyples@laurentian.ca (N. Cyples)

2.1 Abstract

Located in south-eastern British Columbia, the Kicking Horse River is an 80 km long, gravel-bed, braided tributary of the Columbia River, directly supplied by glacial meltwater from the proximal Wapta and Waputik Icefields in the Canadian Rocky Mountains. Previous studies have established the Kicking Horse River as an ideal model for the conceptualization of proximal braided river systems. These studies documented processes of bar formation and sediment distribution solely from ground observations; however, the subsurface stratigraphy of the river has not been well documented. This has warranted a more integrated approach aimed at characterizing the subsurface architecture of the gravel bars. Shallow geophysical methods such as ground-penetrating radar (GPR)

are a useful tool for characterizing the internal architecture of braided bars, providing key information about the processes responsible for their formation, migration, and reworking. The construction and interpretation of three-dimensional GPR fence diagrams is based on the identification of five distinct radar facies, termed: discontinuous, inclined, planar, trough-shaped, and mounded reflectors. These facies were then related to architectural elements formed by fluvial processes responsible for bar growth and evolution. Subsurface stratigraphy is dominated by multiple stacked channel-fill deposits as well as relatively large-scale inclined reflectors related to step-wise bar accretion. In addition, channel fills are commonly overlain by horizontally stratified beds, indicative of bedload sheet migration. Discontinuous reflectors are prevalent throughout the radar profiles and are interpreted as crudely-stratified deposits produced by bedform migration and stacking. This study highlights the need for the further development of refined three-dimensional GPR models on modern, proximal alluvium, since the understanding of grain size heterogeneity in these kinds of deposits is critical when exploring for aquifers and hydrocarbon reservoirs. Additionally, these GPR models can be employed as analogues to understand the depositional history and stratigraphic signature of ancient fluvial systems.

2.2 Introduction

The depositional record of braided rivers is a dominant fraction of the sedimentary record of continental basins throughout geological time (Rust 1977; Bridge 1993; Bridge and Lunt 2006; Gibling 2006; Reesink et al. 2014; Huber and Huggenberger 2015), and modern rivers with braided-planform configurations abound in source-proximal and high-relief portions of sedimentary basins over a range of climate and tectonic settings (Bluck

1979; Miall 1983; Hickson et al. 2005; Allen and Allen 2005; Sambrook Smith et al. 2010; Ashworth and Lewin 2012). Channel braiding takes place through nucleation, accretion, and dissection of in-channel bars and, as such, the depositional mechanisms of braided rivers can be inferred through examination of their bar morphology and sedimentology. The sedimentary architecture of braided alluvial deposits has been heavily researched over the past six decades (Coleman 1969; Smith 1970; Miall 1985; Miall 1997a, 1997b; Best et al. 2003; Sambrook Smith et al. 2006; Ashworth et al. 2011; Parker et al. 2012; Welber et al. 2012). However, there remains scope for more sophisticated assessments of bedding architecture and grain-size heterogeneity of modern systems, since approaches of this kind aid in the better characterization of hydrocarbon reservoirs and aquifer heterogeneity (Anderson et al. 1999; Bridge and Lunt 2006; Huggenberger and Regli 2006; Bayer et al. 2011), as well as in the identification and characterization of modern analogues for better interpretation of ancient systems (Bridge 1993; Ashworth et al. 2011; Okazaki et al. 2015).

Classic work on modern braided rivers and outcrop equivalents (Williams and Rust 1969; Walker 1976; Smith 1974; Cant 1977; Miall 1977a, 1996; Sambrook Smith et al. 2009; Horn et al. 2012; Okazaki et al. 2015) has established links between the planform evolution and stratigraphic signature of low-sinuosity fluvial systems, and provided reliable facies models in one and two dimensions (e.g., vertical logs and lateral sections) (Sambrook Smith et al. 2005). However, more refined models aimed at predicting three-dimensional facies distribution require integrated approaches not solely based on ground observations. Shallow geophysical methods including ground-penetrating radar (GPR) have been used increasingly by fluvial geomorphologists and sedimentologists to map

channel deposits and floodplain structure in two and three dimensions (Jol and Bristow 2003; Sambrook Smith et al. 2006; Mumpy et al. 2007). The use of GPR allows for the depiction of high-resolution subsurface bedding architecture based on contrasts in electrical properties seen in water and sediment composition (Davis and Annan 1989) and is favorable in granular materials such as those composing sand- and gravel-dominated fluvial systems (Huggenberger 1993; Bristow et al. 1999; Best et al. 2003; Mumpy 2007; Hickin et al. 2009). The application of GPR in conjunction with sequential remotely sensed analyses of satellite and aerial imagery links patterns of morphodynamic change in planform style to detailed three-dimensional subsurface profiles (Bridge et al. 1995; Lunt et al. 2004; Bridge and Lunt 2006; Horn et al. 2012a, 2012b).

A number of mature braided river systems with well-developed depositional models have now been assessed using GPR and remote-sensing approaches, with notable examples including the Platte and Niobrara rivers in Nebraska (Skelly et al. 2003; Bristow et al. 1999; Horn et al. 2012a, 2012b), the Rio Paraná in Argentina (Sambrook Smith et al. 2009), and the South Saskatchewan River in the Canadian Prairies (Sambrook Smith et al. 2006; Ashworth et al. 2011; Parker et al. 2013). These studies have produced a new generation of depositional models based on GPR and multi-temporal remote sensing that together represent the state of the art for fluvial-braided sedimentation. With a few exceptions such as the Sagavanirktok River of Alaska, these studies, are however, biased towards systems occupying alluvial plains located hundreds of kilometers from their source uplands, therefore leaving a gap in knowledge for more proximally-located and valley-confined braided river systems.

The Kicking Horse River, located in southeastern British Columbia (Canada), is a proximally sourced braided river system, and was first documented by classic sedimentologic work by Smith (1974) and Hein and Walker (1977). This work provided ground observations and related channel pattern to stream flow, but contained no information on subsurface architecture and stratigraphy. Our goal in this study is to present a detailed account of the links between planform evolution and bar sedimentology, as well as taking advantage of GPR imaging of bedding architecture for the Kicking Horse River. We integrate ground observations with decade-scale multi-temporal satellite imagery and aerial photography, and analysis of discharge records over a 7 km valley-hosted reach located near the town of Field (British Columbia, Canada). Specific objectives of this study are: (i) to examine the morphodynamic evolution of mobile channel-bar complexes based on the interpretation of multi-temporal imagery as well as observations from ground sedimentology; (ii) to analyze transverse and longitudinal subsurface architectural panels through the identification and interpretation of GPR radar facies; and (iii) to identify/quantify the stratigraphic signature of channel migration and bar construction in relation to planform change.

2.3 Regional Setting

Located in the Rocky Mountains of south-eastern British Columbia (Canada), The Kicking Horse River is an ~80 km gravel-bed braided tributary of the Columbia River (drainage area ~1850 km^2) largely supplied by meltwater of the Wapta and Waputik Icefields (Abaddo et al. 2005). Bedrock in the catchment consists of Cambro-Ordovician dolostone and limestone in the form of thrust sheets (~80% of catchment), with Cambrian quartzite confined to a sub-catchment to the north, near the Yoho River (Smith 1974).

Almost all (~98%) of the sediment load in the Kicking Horse River near Field consists of detritus derived from carbonate rocks (Hein and Walker 1977). Rock-glacier activity and mass wasting processes contribute to the sediment load of the river, with talus slopes commonly occupying valley sides over-steepened by late Pleistocene glacial erosion. The study reach is located less than 5 km from its glacial source (and hence by definition *proximal*) and extends for approximately 7 km adjacent to the town of Field (Fig. 1). The upstream reach is relatively narrow due to valley confinement, but the alluvial plain widens when proceeding downstream. The alluvial plain, consisting of active channels and a sparsely vegetated floodplain, are interrupted in the middle alluvial section by a large alluvial fan, upon which the town centre of Field is built. The alluvial plain is elsewhere confined in places by older river terraces, highway fill, and deposits emplaced by glacial and mass-wasting events.

Upstream of the study reach, substantial railway work included the construction of two spiral tunnels, bridges and embankments along the sides of the Kicking Horse valley several hundred meters above the river (Jackson 1979). This construction has led to slope instability and enhanced mass wasting, triggering major debris flows on four separate occasions (1925, 1946, 1962, 1978). The largest debris flow in 1978 likely resulted from ice-dam failure in a gulch at the base of the nearby Cathedral Glacier. It completely washed out the railway and the adjacent Trans-Canada Highway, depositing 1.75×10^5 m^3 of material into the Kicking Horse River alluvial plain and valley floor. The tunnels have since been restored; however, adjacent slopes still contribute to sediment to the river just upstream of the study reach.

The mean annual temperature is 6°C (Station – 11790J1, 51°26’34N, 116°20’50”W). Summer months (June – September) average 16°C and winter months (December – March) average -9°C. Although higher precipitation events are recorded and have been related to flash floods (i.e. 10-year floods, 100-year floods), total precipitation in the summer averages ~135 mm of rain. In the winter, snow accumulation at the valley bottom can reach values as high as 120 cm.

A complex network of braided channels in the Kicking Horse River alluvial plain undergoes diurnal and seasonal fluctuations in flow because of varying glacial-meltwater supply and runoff recharge. As a result, the highest flood stage of the river occurs in late spring and the early summer months, where most of the sediment transport, deposition and reworking occurs at this time. The nearest gauging station is located ~50 km downstream in Golden, BC (Station - 08NA006, 51°18’04”N, 116°58’19”W)and has recorded water level and discharge along the lower Kicking Horse River since 1912. Maximum annual discharge occurs in June at approximately 180 to 320 m^3/s (Government of Canada - Water Office, 2018). In contrast, low-flood stage (5 to 10 m^3/s) occurs in the winter due to the cessation of glacial melting and accumulation of snow.

2.4 Methods and Terminology

This study integrates ground observations, interpretation of river discharge data, GPR imaging, and remote sensing of high-resolution satellite imagery spanning a period of eight years. Sedimentologic observations were made on bar surfaces at low discharge in August 2016. A total of 387 GPS-referenced stations across ten fluvial bars were established to characterize variation in bed material size through both mean and largest

grain size, as well as local flow direction, vectors of bars accretion, and vegetation cover (Fig. 2). These data were compiled and mapped using ESRI^{TM} ArcGIS software and then combined with remote sensing and GPR data (see below). Ordinary kriging was used to interpolate values and map the spatial distribution of flow-divergence values, which is defined as the angle between flow and accretion direction over a bar flank (cf. Jablonski 2012). Pragmatically, the degree of vegetation cover was visually estimated based on the percentage of vegetated soil, grassland, and old-growth vegetation (in four classes 1 through 4 representing 25% increments).

The terminology used to describe the braided planform is adapted from Williams and Rust (1969), Smith (1974), Bridge (1993), and Ielpi and Rainbird (2015) and emphasizes the distinction between fluvial morphological elements (i.e. bars and channels). The distinction between different types of braid bars is dependent on the location of the channel banks and the channel itself. *Side bars* refer to braid bars that accrete downstream and are attached an accretionary bank on one side only, while *mid-channel bars* form in response to channel braiding and are bound on either side by active channels. The term unit bar refers to an elemental and relatively unmodified bar created mainly through accretionary deposition given by the paleoflow direction of observed bedforms and/or clast imbrication. The main channel in the alluvial plain is identified based on the widest hydraulic cross-section, while anabranch channels or ‘secondary’ channels carry flow diverted from the main channel and are typically active during higher-flow stages. The channel belt consists of all active channel-bar complexes and inactive channel fill deposits, while the alluvial plain encompasses the channel belt and adjacent floodplain.

2.4.1 Remote Sensing

Changes in river channel and bar configuration were captured using a combination of aerial photography and high-resolution GeoEye-1™ satellite imagery (with variable ground resolution of 0.46 m to 15 m), which was obtained using the multi-temporal analysis tool in Google™ Earth Pro software. Images were selected for September 2004, August 2010, September 2010, and May 2012 covering an eight-year time period, and to capture the river's planform and flow stage during a variety of seasons. These scenes contain cloud-free coverage and were acquired within 5˚ of nadir. The river has lower flow in September 2004 and August 2010 and higher flow in September 2010 and May 2012. Annual hydrograph plots were prepared for the years in which remotely sensed imagery was available. The images were imported into Adobe™ Illustrator software and the main channel, anabranch channels, mid-channel bars and side bars were delineated for the different times. Adobe™ Photoshop was used to estimate the relative area of each surface type (i.e. bar and channel) using false-coloring and selective pixel-counting procedures.

2.4.2 Ground-Penetrating Radar

Ground-penetrating radar (GPR) work was conducted in October 2016, under low-flow conditions using a PulseEKKO Pro GPR system (Sensors & Software Inc.). A grid pattern with line spacing of 30 m was chosen for five braid bars; the most detailed survey conducted on Bar #1, midstream of the study reach and confined by the alluvial fan (Fig. 2, Fig 3). Four side bars and one mid-channel bar were surveyed along longitudinal and transverse lines (Fig. 2, Fig. 3) totaling nearly 3800 m of survey data. Results reported in this study used 100 MHz antennae and a 1000 V transmitter setting. The antennae were

arranged perpendicular to the GPR transects with a fixed spacing of 1 m and data collected using a step size of 0.25 m. Separate common-mid-point (CMP) surveys were used to estimate an average radar wave velocity of 0.07 m/ns resulting in a nominal vertical radar resolution of ~0.25 m. An engineering level was used to determine surface elevation along transects and a topographic correction was applied to the radar profiles. Data editing and signal processing were carried out using EKKOView™ Deluxe software and included dewow, bandpass filter (to reduce high and low frequency noise) and depth conversion. Processed images were interpreted, and radar facies were then delineated using Adobe™ Illustrator. A selective pixel-count analysis was again used to quantify the relative abundance of each radar facies.

2.5 The Kicking Horse River at Field, British Columbia

2.5.1 Alluvial geomorphology

The study reach can be divided into three distinct geomorphic reaches, respectively, upstream, midstream, and downstream. A reach is a length of channel that displays similar physical characteristics. Reaches were delineated based on similarities in fluvial processes, topography, valley setting, and hydrology. Ten bars selected for detailed study (Fig. 2, Fig. 3), three (3) in the upstream reach, five (5) in the midstream reach, and two (2) in the downstream reach. We observed these reaches to determine how they differ with regards to spatial confinement, slope gradient, channel-belt width, channel style, type of bars and their internal morphologies, sediment grain size, and vegetation cover. The alluvial plain is bound by the Trans-Canada Highway on its hydrographic right and the midstream portion of the alluvial plain is restricted by the alluvial fan upon which the town of Field is built.

The upstream reach of the alluvial plain has a down-valley gradient ranging between 0.97% and 1.53% and occupies a valley 600-1200 m wide (Fig. 4). The active channel belt ranges in width from 180 m to 425 m, with the widest portion being the floodplain. Across-valley gradients range between 0.13% and 0.26% and are steepest towards the northwest (Fig. 4B). Mid-channel bars up to 200 m in length and 55 m wide as well as small, individual unit bars that have coalesced to form compound side bars are prevalent throughout the reach. Many of these bars are dissected by minor cross-bar and chute channels that form when the river floods. Upstream bar surfaces consist of relatively coarse sediment (10% cobbles, 70-80% pebbles, and 10-20% coarse-grained sand) and are characterized by 25-50% vegetation cover (Fig. 5A, 5B). The highest density of vegetation is observed in the upstream reach where topography is elevated (Fig. 5B). The active channel belt consists of a main low-sinuosity channel 15 m – 50 m in width, flanked by subordinate anabranch channels 1 m – 10 m in width. These secondary channels are more sinuous than the main channel and host numerous, smaller mid-channel bars (Fig. 6). Rates of flow divergence are typically less than 30° (Fig. 5C).

In the midstream reach of the river, the degree of channel braiding increases substantially as do flow divergence values ranging from 30° - 60° (Fig 5C). The channel belt widens to ~450 m, except where it is constrained (width ~60 m) by alluvial fan development adjacent to the Field Townsite. Active anabranch channels siding the main channel are more common in the midstream reach with secondary channels hosting a relatively high number of larger mid-channel bars. Widths of the main channel range between 12 m and 25 m, while anabranch channels are as wide as ~12 m. Topographic confinement

decreases as the valley opens and down-valley gradients are much gentler (<0.30%). Across-valley gradients are highest through Field at ~2% (Fig. 4B).

Downstream, the channel belt approaches ~300 m and channel braiding is likewise dominant. The reach hosts large, more elongate mid-channel bars, reaching lengths up to 350 m and widths of 100 m. Mid-channel bars are more prevalent than compound side bars and are dissected by cross-bar channels. Bar-top sediment is predominantly medium (60-70%) and fine (30-40%) sand, while vegetation cover remains uncommon apart from Bar #4 (Fig. 5B). The downstream gradient is approximately 0.20% and across-valley gradients vary between 0.36% and 0.80% (Fig. 4B). Finally, the terminal end of the alluvial plain narrows to ~50 m due to valley constriction before connecting downstream to other tributaries.

2.5.2 Discharge records

Discharge records from the gauging station in Golden, BC were used to consider diurnal, seasonal, and annual streamflow of the Kicking Horse River over the eight years studied (September 2004 to May 2012). The river flows continuously through the year with annual peak discharge averaging ~240 m^3/s, and the highest peak flow recorded in June 2007 and 2012 at 330 m^3/s. The lowest flow observed at Golden is ~5 m^3/s between January and March. As expected, the regular glacial flow regime is observed, where seasonal peaks are observed in the summer months (June and July) due to persistent glacier melt, resulting from increased temperatures (Fig 7) (Government of Canada - Water Office, 2018). Diurnal fluctuations of 15 to 40 m^3/s are recorded in the summer in June and July in response to daytime ice and snow melt. In the winter, discharge is

significantly reduced from the onset of cool temperatures and remains relatively constant around 5 -10 m^3/s from December to March.

Satellite images from September 2004, August 2010, September 2010, and May 2012 were used to illustrate differences in planform of the river at various flow stages. The September 2004 image represents a low-flow stage (30 m^3/s at Golden) following atypical (end of July) summer flow rates, where the river was transitioning to a low flow. Peaks above 60 m^3/s are observed lasting only a couple days at a time likely from large precipitation events, before tapering off to below 20 m^3/s into the fall months with cooling temperatures. In August 2010, the river had a discharge of 50 m^3/s (at Golden), whereas by September 2010 the river discharge had more than doubled (Fig. 7). This anomalously high discharge is attributed to a large rainfall event (>30 mm in one day) that had just impacted the river's catchment basin. Finally, in May 2012, the river had an elevated spring discharge of 95 m^3/s (Fig.7). In the preceding months, the river was at its seasonal low flow of 5 to 10 m^3/s before discharge rose in May due to the onset of glacial melting as temperatures rose well above freezing.

2.5.3 Channel Belt Planform

Changes in planform were captured across an eight-year timespan using aerial snapshots to examine the rates of change and areal extent over which the braided channels migrate, and to test whether migration events displayed any relationship with specific flow stages of the river. Upstream, channels abandoned from previous stepwise migration events indicate a lateral migration to the hydrographic right of the channel at an average rate of 9 m/year (~72 m total). In contrast, downstream imagery displays the largest rates of planform shift between September 2004 and September 2010, where the channel belt is

subject to high flood stage. Over these six years, the downstream reach of the main river channel shifted from one side to the other, spanning the entire width of the channel belt from its hydrographic left to right (~275 m of lateral migration recorded, accounting for an average rate of 34 m/year).

Within the main channel, notable change in the extent and distribution of bars was evident over the eight-year timespan (Fig. 6). Both mid-channel and compound side bars are observed, and their relative abundance varies spatially (i.e. upstream vs downstream) and temporally on both yearly and seasonal scales due to variations in channel geometry arising from fluctuations in discharge. Bars are gravel-dominated upstream and sand-dominated downstream and consist of both erosional and depositional morphologies which are dependent on the flow regime (cf. Ashley 1990). When discharge is high (i.e. September 2010 and May 2012), mid-channel bars dominate 60-70% of the alluvial plai (Fig. 8). Previously large, compound mid-channel bars become more abundant when dissected by numerous anabranch channels, formed from an increase in flow and subsequent channel bifurcation. These bars are subject to high rates of erosion and reworking while flow is high, a process also promoted by the lack of stabilizing vegetation (i.e. <25%) and cohesive sediment (Schumm 1968; Gran and Paola 2001; Murray and Paola 2003; Tal and Paola 2010).

At low-flow stage in September 2004 and August 201, compound side bars are better exposed and compose a dominant fraction of the alluvial-plain surface area. The largest side bars are constructed through various cycles of sediment deposition, accretion, reworking, and channel avulsion as discharge fluctuates. More specifically, growth of side bars begins with the preferential downstream accretion of small unit bars, followed

by further asymmetric growth as the bars enlarge (Fig. 9). Bar development and migration can also be facilitated by the reactivation of abandoned channels in which bars become dissected. Final stages of growth as bars reach several hundred meters in length are characterized by a much wider main channel, where additional unit bars form on the central upstream side of the alluvial reach (Fig. 9). Approximately 55% to 65% of the total bar surface consists of side bars (Fig. 8), while the area of the active channel surface decreases significantly as anabranches become inactive and the width of the main channel narrows. At low flow, especially in the winter, bars remain relatively unmodified due to minimal discharge in the channels.

Changes in bar formation, channel migration, and sediment transportation are also observed across a timespan of just 8 to 10 hours. In the early morning hours of a daily discharge cycle, when water level is relatively low, numerous gravelly mid-channel bars are exposed (Fig. 10A). After ten hours, mid-channel bars become nearly fully submerged as the daily discharge reaches its maximum (Fig. 10B). Additionally, side bars are flooded when discharge is high, creating lateral accretion surfaces in the direction of channel migration (in the case illustrated, towards the hydrographic right) (Fig. 10B).

2.6 Radar Facies

In this study, five key radar facies have been recognized in GPR longitudinal and transverse profiles across five bars (Fig. 11). Facies are defined through the recognition of distinctive patterns of reflectors that mimic bedding architectures and can be related to specific processes and/or architectural elements responsible for bar construction and

degradation. On average, the depth of penetration where discernable reflectors can be identified is 6 m – 7 m, however, radar facies have only been delineated above 5 m in depth, the maximum depth at which a prominent and continuous reflector is observed across all the imaged profiles (Fig. 12A, 12B). The base of this boundary is interpreted as the bottom of the active channel belt.

2.6. 1 Facies 1 - Discontinuous Reflections

Description.— Radar Facies 1 is the most prevalent facies observed, and is characterized by discontinuous reflectors that are wavy to undulatory. Reflections may be wavy and laterally continuous for tens of meters or grouped into small trough-shaped features that are more limited in extent (i.e. < 5 m) (Fig. 12A, 12B). These troughs are typically truncated by reflections of other radar facies. Packages of discontinuous reflections occur at a variety of depths in the radar profiles. Radar Facies 1 is more prevalent (> 50%) in across-stream (transverse) 2-D transects measured perpendicular to stream flow direction. In downstream-oriented transects, Facies 1 is less abundant (30-50%). The relative abundances of Facies 1 are presented in *Figure 13.*

Interpretation.— Discontinuous reflections are interpreted as crudely-stratified sandy and gravelly beds produced by the migration of bedforms, most likely dunes 1-2 m in height (Sambrook Smith et al. 2009). This migration of bedforms is also likely responsible for the construction of small-scale unit bars. Laterally continuous reflections are indicative of vertical accretion on bar tops when little forward migration is occurring. Similar bedforms as well as more horizontal variants have been observed by Mumpy et al. (2007) in a sandy braided bar in the Wisconsin River. The abundance and variable depth of Facies 1 can be attributed to the dynamic discharge regime of the river and the

proximity of the study reach to its glacial source, and could be related to diurnal fluctuations in river discharge. Also, most transverse GPR transects were measured perpendicular to flow, an orientation that is probably the most favorable for easy recognition of bedform-scale architectural forms.

2.6.2 Facies 2 - Inclined Reflections

Description.— This radar facies consists of sets of dipping reflections ranging in inclination between 5˚ and 20˚ (Fig. 12A, 12B). Packages of inclined reflections are up to 2 m thick and contain beds of 0.5 m to 2 m. Reflections commonly occur as lenses and are laterally continuous for up to 40 m. Radar Facies 4 frequently truncates packages of inclined reflectors laterally, while Radar Facies 3 frequently truncates them at the top. Inclined reflections are most abundant in the midstream to downstream reaches of the channel belt. In downstream-oriented GPR transects, Radar Facies 2 represents 5-10% of all reflections in the bars in the upstream reach of the river, whereas in the midstream and downstream reaches, they represent 20-30% of reflections (Fig. 13B). In transverse transects, inclined reflections vary in abundance up to 15%, regardless of their upstream/downstream location in the channel belt (Fig. 13A). This facies is most prevalent at depths of 0-3 m.

Interpretation.— Steeply-dipping reflections are indicative of coarse-grained foresets produced by the advancement of avalanching fronts during a formative discharge event. During high flow stages, the deposits of existing bars are overtopped with sediment that avalanches down the slipface (downstream end of the bar), depositing sediment at high angles as the bar enters deeper waters (Ashworth et al. 2000; Lunt et al. 2004; Sambrook Smith et al. 2005; Rice et al. 2009; Ashworth et al. 2011). This

interpretation is consistent with earlier work on this reach of the Kicking Horse River conducted by Smith (1974) and Hein & Walker (1977). The thickest sets, accordingly, are observed in those locations where bars migrate into channel thalweg (Sambrook Smith et al. 2005). The generation of steep bar-margin slipfaces is likely favored by the coarse-grained nature of the alluvium. In the examined GPR profiles, the steepest reflectors are truncated by other radar facies, and likely represent bar margins. Lower angled inclined reflections represent instead small-scale downstream accretion surfaces produced from the migration of lower-relief bars. Entire packages of both high and low angle reflectors likely represent avalanching fronts of individual unit bars (Okazaki et al. 2015).

2.6.3 Facies 3 - Horizontal Reflections

Description.— Radar Facies 3 consists of continuous horizontal to sub-horizontal reflections that are laterally continuous for up to 120 m in longitudinal sections and up to 50 m in transverse sections (Fig. 12A). Reflections are parallel to sub-parallel and are seldom truncated by other radar facies. Horizontal packages tend to be concentrated close to the bar surface (< 2 m depth) and most commonly occur in the most upstream reach of the alluvial plain, as well as in the upstream section of individual bars. In longitudinal profiles, approximately 20-50% of reflectors are horizontal, while in transverse profiles only 5-10% of reflectors are horizontal (Fig. 13A, 13B).

Interpretation.— This facies is interpreted as aggrading bar top sheets, as found in other gravel-bed systems such as the lower Fraser River (Rice et al. 2009) and the Sagavanirktok River (Lunt & Bridge 2004). Such bedload sheets are developed at high flow stage and represent downstream migrating, coarse traction carpets (Hein & Walker

1977; Whiting et al. 1988; Bridge 1993; Bridge 2006). Bedload sheets are not often truncated, i.e. they show no sign of reactivation. Where subsidence and burial occur, stacked bedding becomes more irregular and less parallel (Rice et al. 2009). The abundance of Radar Facies 3 in the upstream reach of the channel belt, as well as in the upstream portion of individual bars can be attributed to the development of upper-flow regime plane beds that eventually lead to the deposition of bedload sheets. In the upstream region of the alluvial plain, most of the discharge is focused into a single channel, a setting that facilitates the configuration of coarse-grained, upper-flow regime plane beds.

2.6.4 Facies 4 - Trough-Shaped Reflections

Description.— Radar Facies 4 is characterized by small to large-scale (5 m- 50 m) concave-upwards reflections, resembling troughs. Facies 4 commonly truncates inclined reflectors of Facies 2 laterally and is commonly overlain by horizontal reflections of Radar Facies 3 (Fig. 13B). Radar Facies 4 is observed at various locations within the alluvial plain and is most frequently observed within the upper 4 m of the deposits. Individual trough features range from 1 m to 4 m thick and extend laterally up to 50 m. This facies is more common in transverse transects (20-50%) than longitudinal sections (5-10%) (Fig. 13A, 13B).

Interpretation.— Concave-upwards reflectors are indicative of channel fills at a variety of scales and their thickness directly relates to formative-flow depth in paleochannels (Sambrook Smith et al. 2006; Ashworth et al. 2011). Most radar profiles in this study contain multiple channels stacked, likely indicating the development of multi-storey channels (Rice et al. 2009). These stacked channel fills are produced from repeated

episodes of cut and fill associated with fluctuations in seasonal discharge (high flood vs. low flood). There is evidence for channel abandonment and reactivation where Facies 4 channel fills are truncated on the side by Radar Facies 2 (inclined reflections).

2.6.5 Facies 5 - Mounded Reflections

Description.— Radar Facies 5 consists of isolated hyperbolic or mounded reflections. They have been observed in most bars 1 – 4 m from the bar surface, but are only apparent in transverse profiles (Fig. 12B). This facies is the least common, accounting for only 5-15% of profiles where it is identified (Fig. 13A).

Interpretation.— Mounded reflections likely represent buried debris, such as logs. Parabolic reflections of buried objects occur in GPR profiles where unshielded antennae transmit/receive signal in all directions and are detected before and after the survey passes over them. During high flow, woody debris (such as tree trunks) eroded from channel banks or stranded on bar tops is entrained within the channels, transported downstream, and eventually buried by other bedforms. Since these reflections do not appear in longitudinal profiles, some of them could also be the product of individual, high-relief transverse unit bars dug out and replaced by an out-sized clast.

2.7 Discussion

A dynamic discharge regime in conjunction with low bank stability allows for the rapid planform change of braided rivers (Thorne et al. 1993; Coulthard 2005; Horn et al. 2012). Numerous studies on both modern (Miall 1977; Cant and Walker 1978; Ashworth et al. 2007; Horn et al. 2012) and ancient (Gibling et al. 2010; Ielpi and Ghinassi 2015; Ghinassi and Ielpi 2018) fluvial-channel belts have shown that braided rivers typically

undergo landscape change in response to distinct hydraulic cycles and associated variations in sediment supply. These cycles have three characteristic stages developed through episodic aggradation and erosion, beginning with: (1) a high flood stage with low sediment supply, where the alluvial plain is subject to substantial erosion, resulting in channel undercutting and bar erosion, followed by (2) an early waning flood stage where discharge and sediment are in dynamic equilibrium, depositing large foreset bars, and lastly (3) a low flood stage, where the margins of larger compound bars get reworked into smaller bars that remain until another flood event reinitiates the cycle, or channel avulsion occurs. Repeated discharge cycles are postulated to influence the response of bar and channel forms in both the planform and subsurface of the Kicking Horse River and are discussed below.

2.7.1 Depositional Model

Planform morphodynamics and subsurface stratigraphy obtained from ground-penetrating radar analysis provides insight into the depositional mechanisms of the Kicking Horse River near the town of Field, British Columbia. Three-dimensional depositional models of the river alluvium may reveal key relationships between sedimentary processes and the preservation potential of architectural elements, which are a crucial aspect for the analogue modeling and interpretation of sedimentary architecture and facies of ancient fluvial systems. *Figures 14A, 15A, and 16A* illustrate the distribution of radar facies in 3-D for three bars located within various reaches of the alluvial plain. In this study, ground-penetrating radar (GPR) revealed three distinct architectural elements based on the different radar facies: bedload sheets, channel fills, and unit bars. The distribution of architectural elements is displayed in *Figures 14B, 15B, and 16B*, highlighting the

variability in abundance across a variety of bars. Additionally, five main depositional processes were recognized based on the integration of subsurface data and planform observations: (1) vertical aggradation on bar tops; (2) bedload sheet migration and bypass on bar tops; (3) outbuilding of bar flanks; (4) channel abandonment and reactivation; and (5) small-scale vertical and lateral accretion of individual bedforms. These processes and associated deposits are discussed hereafter for three reaches of the Kicking Horse River's alluvial plain, based on their morphodynamics and depositional style.

Upstream Reach

Bedload sheets dominate the upstream reach of the channel belt based on three-dimensional architectural reconstruction of GPR profiles. Average grain size is coarser, with approximately 80% - 90% of the upstream bars consisting of large pebbles and cobbles (Fig. 5A). Flow is confined into a deep, main channel flanked by few secondary anabranch channels representing active drainages during rising- to peak-flood stages capable of entraining coarse bedload material (Fig. 6). Bedload sheets are ~50 m – 150 m wide and 1 m – 3 m thick (Fig. 14A, 14B) and the high preservation of these gravel-dominated sheets is attributed to the low degree of sediment reworking in abruptly falling hydrograph levels following a formative discharge event. Vegetation coverage higher than elsewhere in the alluvial plain, which in addition to coarse-grained bank material in the upstream reach (25% - 50%) (Fig. 5B), may help in stabilization of the main channel as evidenced in other studies (Schumm 1968; Gran and Paola 2001; Tal and Paola 2007; Ielpi 2017). This limits channel braiding and lateral migration to some degree (Smith 1976; Huisank et al. 2002). Lateral stability of a channel belt is also controlled by valley confinement and sediment supply (Schumm 1985). The planform is restricted from

widening and braiding since valley confinement is high and sediment supply is relatively low (Charlton 2008). This is illustrated in *Figures 4A, 4B, and 4C*, where topographic profiles of the Kicking Horse River are provided.

Low rates of both flow divergence (i.e. < 30°) and channel sinuosity in the upstream reach minimize processes of channel reactivation and abandonment, as seen in GPR profiles by the lack of channel fills. This aspect is related to the occurrence of a dominant flow structure in the down-valley direction near parallel to the channel-belt axis, again as a result of high valley confinement that inhibits extensive lateral migration (Fig. 4C) (Jones and Schumm 1999). One large ~20 m wide channel fill is preserved beneath Bar #3 indicating the entire bar was once transected by a large migrating channel, likely what used to be the main channel of the river (marked as radar facies 4 on Fig. 14A, Fig. 14B). The low degree of anabranching currently seen upstream (Fig. 6) is consistent with the low number of preserved smaller channel fills in the GPR sections (Fig. 13A, 13B). Rates of channel migration calculated from satellite images from 2004 to 2012 average ~4 m/year, although it is possible this is a result of channel braiding from flood events as opposed to proper accretionary migration. Overall, increased valley confinement and the high abundance of vegetation reduces the relative number of active channels and results in lower rates of channel migration (Gran and Paola 2001).

At high discharge and low sediment supply, downstream accretion of compound-bar sheets is most common upstream, while lateral migration and bar stabilization is minimal (Ashworth 1996). Bars are partially or entirely submerged or occasionally dissected by smaller channels as flow rises, such that small mid-channel bars with gently-dipping inclined strata are preserved. The steep banks of bar heads erode first (Rust 1972; Miall

1977), entraining downstream-bypassed bedload. Preserved bars in GPR data are typically no longer than ~20 m and no wider than 2 – 3 m (Fig. 14A, Fig. 14B), and suggest a high flood stage, where only smaller mid-channel bars are preserved as the flow dissects the previously deposited larger bars. As an exception to what is stated above, one bar ~50 m long in the downstream direction (marked as radar facies 2 in Fig. 14A) is preserved within the subsurface profiles, likely representative of a compound side bar that amalgamated and stabilized during a waning flow.

Midstream Reach

Midstream, the alluvial plain of the Kicking Horse River widens substantially to approximately 450 m, facilitating bar growth and channel braiding due to decreased spatial confinement as well a 25% reduction in vegetation cover (Fig. 4B, Fig. 5B) (cf. Hey and Thorne 1986; Millar 2000; Coulthard 2005). Flow expansion in shallower and wider channels, together with vertical accretion of unit bars may also trigger episodes of channel braiding (Ashmore 1993). High rates of channel braiding and anabranching are especially evident in remote sensing images for September 2010 and May 2012, where ~30% – 50% of the alluvial plain contains active channel-bar complexes. Lateral accretion of bars is a common depositional mechanism midstream based on evidence of bar accretion that is transverse to the local flow direction. Proper accretionary channel migration is observed midstream from satellite imagery averaging a rate of 9 m/year. Increased mobility of channels is related to the high abundance of channel fills preserved in GPR profiles in addition to smaller mid-channel bars (Fig. 15A, 15B). Large barforms resembling compound side bars are not as easily preserved in the subsurface when channel braiding is more extensive as portions of side bars are easily dissected by

anabranch channels and then isolated as mid-channel bars. However, the record of channel abandonment and reactivation are frequently preserved in GPR profiles, and is shown through evidence of bars being directly in contact with their parent channels, where channel fills are directly in contact with deposits of unit bars (Fig. 15B). Evidence of highly-inclined slipfaces at bar margins are interpreted as avalanching fronts developed from an increase in sediment supply coupled with channel undercutting of the bar tails as described by Sambrook Smith et al. (2009). The occurrence of bars in contact with their parent channel also suggests the formation and subsequent reworking of mid-channel bars where channel bodies are observed on either side.

Ultimately, the abundance and geometry of channels is controlled by net sedimentation, channel migration and frequency of channel avulsions (Allen 1965; Allen 1978; Miall 1996). Flow divergence increases in the midstream reach to an average of ~120° midstream, indicating that channels attain a low to intermediate sinuosity before their bars undergo braiding and dissection as evidenced by Jones and Schumm (1999). The slight increase in channel sinuosity is favored by the gradient of the channel belt, which decreases from ~1.5% to ~0.30% (Fig. 4A, 4B, 4C), in addition to the widening of the alluvial plain, which limits lateral confinement (cf. Ferguson and Ashworth 1991; Lazarus and Constantine 2013; Ielpi 2017).

Downstream Reach

Substantial planform evolution and channel mobility is also observed in the downstream reach, where the alluvial plain has lower channel belt topography. The largest rate of lateral migration is observed downstream, approximating ~34 m/year (for a total of 273

m over 8 years) (Fig. 6), although it is likely the sharp shifts are attributed to increased braiding from individual flood events. Sediment transport is reduced as the slope decreases and the valley widens, resulting in the immobility of bars and channels (Rust 1972; Hey and Thorne 1986). Bars are dominated by large inclined packages representing compound bars, formed from the amalgamation and accretion of unit bars that are deposited as discharge and flow competence decreases, and as the river transitions into a low-flood stage (cf. Ferguson and Ashworth 1991; Bristow and Best 1993; Rice et al. 2009). In the Kicking Horse River, the channel belt becomes shallower, where bars are subaerially exposed and the margins are reworked by migrating secondary channels during waning flow. This is also observed by Ielpi and Ghinassi (2015). Bars become more isolated and grow in length as flow diminishes and diverts downstream. Gently-dipping cross strata on bar margins likely represent areas where sand accumulates and represents the outbuilding of bar flanks (Ghinassi and Ielpi 2018). Values of flow divergence average 30 – 50° (Fig. 5C) and increase until bars emerge or get dissected (Ashworth 1996). Modern channels evident from remote sensing are significantly smaller in size than their upstream counterparts, and this is consistent with what observed from GPR profiles, where solely small channel fills, likely representing anabranch channels, are preserved. This is supported by the high degree of channel anabranching and presence of narrower channels in response to smaller grain size and lower bedload transport.

Prolonged reworking of lateral bar surfaces occurs as the river is more often at a lower flood stage, therefore high flood stage elements (i.e. bedload sheets) are more extensively reworked and not as well preserved (Jones 1977). The low degree of confinement, in addition to minimal vegetation cover (i.e. < 25%), promote reworking of the alluvial

plain, therefore an abundance of small-scale bedforms including sets of ripples and cross-beds are more commonly preserved (Schum 1968; Smith 1976; Murray and Paola 2003; Ielpi et al. 2016). Ripples and dunes migrate along bar flanks, and occasionally bar tops, at shallow depths during flood weakening until bars becomes dissected and isolated. In 3-D GPR models, this is shown through the high abundance of discontinuous reflectors preserved (Fig. 16A, 16B), representing dune-scale bedforms.

2.7.2 Comparison with Other Studies

As a caveat fot the depositional models discussed here, GPR-based analyses can only depict a small portion of geological time represented by alluvial records, and cannot fully illustrate the entire morphodynamic evolution of an alluvial system. That being said, patterns of braid-bar growth and channel migration in the upstream reach of the Kicking Horse River show key similarities with those observed in other gravel-dominated braided systems (Miall 1977; Bridge 1993; Lunt and Bridge 2004; Bridge and Lunt 2006), while the midstream and downstream reaches are more akin to sand-richer systems (Best et al. 2003; Skelly 2003; Sambrook Smith et al. 2005; Sambrook Smith et al. 2006) and/or rivers that exhibit transitional braided to wandering planform (Wooldridge and Hickin 2005; Hickin et al. 2009; Rice et al. 2009).

Bridge and Lunt (2006) suggest dimensionless geometries of bedforms and architectural elements that are abundant within braided rivers of varying scale. One common architectural element is diffuse gravel sheets (Hein and Walker 1977), also referred to as migrating bedload sheets (Whiting et al. 1988), which are an important architectural feature in the upstream of the Kicking Horse River and appear to be the important component of the depositional record at a high-flood stages. Interpreted GPR profiles

highlight the lateral continuity of these horizontal packages, bearing in particular similarities with the results of Lunt and Bridge (2004) and Lunt et al. (2004) from the proximally located and gravel-dominated braid bar in the Sagavanirktok River of Alaska. As in the Kicking Horse River, bedload sheets described in the Sagavanirktok River are particularly abundant along bar tops and record higher-flood stages.

Results stemming from the interpretation of a three-dimensional depositional model of bars midstream and downstream in the Kicking Horse River (Fig. 16A, 16B) also bear many key similarities in depositional style to modern sandy braided rivers (Best et al. 2003; Skelly et al. 2003; Ashworth et al. 2007; Ashworth et al. 2011; Parker et al. 2013). In the downstream reach, all GPR profiles are dominated by the presence of discontinuous reflectors as documented in the South Saskatchewan River. Ashworth et al. (2011) suggested that the high abundance of discontinuous reflectors observed from GPR profiles in the South Saskatchewan River is a product of the migration of small dunes. Similar discontinuous reflectors dominate > 50% of the subsurface in the Kicking Horse River and while they are likely a product of dune migration, we infer that they are also a result of diurnal fluctuations in discharge related to glacial-fed discharge.

Small to medium-scale cross-stratification increasingly dominates bar profiles downstream as found in past studies on modern sandy braided and sand-gravel wandering fluvial systems (Cant and Walker 1978; Sambrook Smith et al. 2009; Horn et al. 2012); however, larger-scale bar-margin slipfaces are also preserved, highlighting the importance of slipface accretion due to avalanching processes in all portions of the Kicking Horse River's alluvial plain (Best et al. 2003; Wooldridge and Hickin 2005). These large-scale inclined faces are much less prevalent upstream, where the ratio

between sediment accumulation and bypass is low. The higher proportion of preserved bar slipfaces in the downstream, lower-gradient and sand-rich reaches of the Kicking Horse River is comparable with what observed in bars of much larger and distal river reaches, such as the South Saskatchewan River (Sambrook Smith et al. 2006a) and the Jamuna River (Best et al. 2003). All in all, the comprehensive Kicking Horse River facies architecture suggests that large bar-margin slipfaces are also an important component of proximally-located and high-gradient braided river systems.

2.8 Conclusions

This research presents an integrated depositional model of the Kicking Horse River, linking changes in planform depicted through remote sensing and ground observations to subsurface stratigraphy resolved through ground-penetrating radar. Remote sensing highlights rates of lateral migration as high as 9 m/year upstream, and 34 m/year downstream where less confined alluvial plain is subject to increased planform adjustment and widening. Large side bars are preferentially developed and preserved at low-flow stage, while smaller mid-channel bars dominate the planform in addition to an abundance of active anabranch channels during high-flow stages. Limited vegetation in addition to the dynamic and fluctuating discharge regime of the Kicking Horse River allows for the rapid changes observed in its planform.

Three-dimensional depositional models of the river alluvium reveal key relationships between sedimentary processes and the preservation potential of architectural elements, which is a crucial aspect for the analogue modeling and interpretation of sedimentary architecture and facies of ancient fluvial systems. In this study, ground-penetrating radar

(GPR) revealed three distinct and elemental architectural features: bedload sheets, channel fills, and unit bars.

The depositional architecture described in this study bears many similarities to other modern and ancient fluvial systems. The upstream reach of the Kicking Horse River more closely resembles other gravel-bed braided systems, while the downstream reaches exhibit similarities to more sandy-gravel rivers that are transitional from braided to wandering in planform. This research presents one of a few integrative studies on a proximally-sourced, glacier-fed, gravel-bed braided river and helps fill a gap of knowledge in facies models of modern braided river systems. There is a need for further studies from a range of other modern braided rivers integrating GPR to help form relationships between alluvial architecture and planform morphodynamics.

2.9 Acknowledgements

This work is part of the M.Sc. project of the lead author and was supported by a Discovery Grant from the Natural Sciences and Engineering Research Council of Canada.

2.10 References

Abbado, D., Slingerland, R., and Smith, N.D., 2005, Origin of anastomosis in the upper Columbia River, British Columbia, Canada, *in* Blum, M.D., Marriott, S.B. and Leclair, S.F., eds., Fluvial Sedimentology VII, International Association of Sedimentologists, Special Publication 35, p. 3-5.

Allen, J.R.L., 1965, A review of the origin and characteristics of recent alluvial sediments: Sedimentology, v. 5, p. 89-191.

Allen, J.R.L., 1978, Studies in fluviatile sedimentation: an exploratory quantitative model for the architecture of avulsion-controlled alluvial sites: Sedimentary Geology, v. 21, p. 129-147.

Allen, P.A., and Allen, J.R.L., 2005, Basin analysis principles and applications, Hoboken, New Jersey, 2nd Edition, Blackwell Publishing, 562 p.

Anderson, M.P., Aiken, J.S., Webb, E.K., and Mickelson, D.M., 1999, Sedimentology and hydrogeology of two braided stream deposits: Sedimentary Geology, v. 129, p. 187-199.

Ashley, G.M., 1990, Classification of large-scale subaqueous bedforms: a new look at an old problem: Journal of Sedimentary Petrology, v. 60, p. 160-172.

Ashmore, P., 1993, Anabranch confluence kinetics and sedimentation processes in gravel-braided streams, *in* Best, J.L., and Bristow, C.S., eds., Braided Rivers, Geological Society of London, Special Publication 75, p. 129-146.

Ashworth, P.J., 1996, Mid-channel bar growth and its relationship to local flow strength and direction: Earth Surface Processes and Landforms, v. 21, p. 103-123.

Ashworth, P.J., Best, J.L., Roden, J.E., Bristow, C.S., and Klaassen, G.J., 2000, Morphological evolution and dynamics of a large, sand braid-bar, Jamuna River, Bangladesh: Sedimentology, v. 47, p. 533-555.

Ashworth, P.J., Best, J.L., and Jones, M.A., 2007, The relationship between channel avulsion, flow occupancy, and aggradation in braided rivers: insights from an experimental model: Sedimentology, v. 54, p. 497-513.

Ashworth, P.J., Sambrook Smith, G.H., Best, J.L., Bridge, J.S., Lane, S.N., Lunt, I.A., Reesink, J.H., Simpson,C.J., and Thomas, R.E., 2011, Evolution and

sedimentology of a channel fill in the sandy braided South Saskatchewan River and its comparison to the deposits of an adjacent compound bar: Sedimentology, v. 58, p. 1860-1883.

Ashworth, P.J., and Lewin, J., 2012, How do big rivers come to be different?: Earth Science Reviews, v. 114, p. 84-107.

Bayer, P., Huggenberger, P., Renard, P., and Comunian, A., 2011, Three-dimensional high resolution fluvio-glacial aquifer analog: part 1 field study: Journal of Hydrology, v. 405, p. 1-9.

Best, J.L., Ashworth, P.J., Sarker, M.H., and Roden, J.E., 2007, The Brahmaputra-Jamuna River, Bangladesh, *in*: Gupta, A., eds., Large Rivers: Geomorphology and Management: Chichester, U.K., Wiley, p. 395-433.

Best, J.L., Ashworth, P.J., Bristow, C.S., and Roden, J., 2003, Three-dimensional sedimentary architecture of a large, mid-channel sand braid bar, Jamuna River, Bangladesh: Journal of Sedimentary Research, v. 73, p. 516-530.

Bridge, J.S., and Lunt, I.A., 2006, Depositional models of braided rivers, *in*: Sambrook Smith, G.H., Best, J.L., Bristow, C.S., and Petts, G.E., eds., Braided Rivers: Process, Deposits, Ecology and Management, International Association of Sedimentologists, Special Publication 36, p. 11-50.

Bridge, J.S., Alexander, J., Collier, R.E. L., Gawthorpe, R.L., and Jarvis. J., 1995, Ground-penetrating radar and coring used to study the large-scale structure of point-bar deposits in three dimensions: Sedimentology, v. 42, p. 839-852.

Bridge, J.S., 1993, The interaction between channel geometry, water flow, sediment transport and deposition in braided rivers, *in*: Best, J.L. and Bristow, C.S., eds., Braided Rivers, Geological Society of London, Special Publication 75, p. 13-71.

Bridge, J., Collier, R., and Alexander, J., 1998, Large-scale structure of Calamus River deposits (Nebraska, USA) revealed using ground-penetrating radar: Sedimentology, v. 45, p. 977-986.

Bristow, C.S., 1993, Sedimentary structures in bar tops in the Brahmaputra River, Bangladesh, *in*: Best, J.L. and Bristow, C.S., eds., Braided Rivers, Geological Society of London, Special Publication 75, p. 163-176.

Bristow, C.S., and Best, J.L., 1993, Braided rivers: perspectives and problems, *in*: Best, J.L. and Bristow, C.S., eds., Braided Rivers, Geological Society of London, Special Publication 75, p.1-11.

Bristow, C.S., Skelly, R.L., and Ethridge, F.G., 1999, Crevasse splays from the rapidly aggrading, sand-bed, braided Niobrara River, Nebraska: effect of base-level rise: Sedimentology, v. 46, p. 1029-1047.

Cant, D.J., 1977, Development of a facies model for sandy braided river sedimentation: Comparison of the South Saskatchewan River and Battery Point Formation *in*: Miall, A.D., eds., Fluvial Sedimentology, The Canadian Society of Petroleum Geologists, Memoir 5, p. 1-47.

Cant, D.J, and Walker, R.G., 1978, Fluvial processes and facies sequences in the sandy South Saskatchewan River, Canada: Sedimentology, v. 25, p. 625-648.

Charlton, R., 2008, Fundamentals of fluvial geomorphology, New York, New York, 1st Edition, Routledge Publishing, 234 p.

Coleman, J.M., 1969, Brahmaputra River: Channel processes and sedimentation: Sedimentary Geology, v. 3, p. 129-239.

Coulthard, T.J., 2005, Effects of vegetation on braided stream pattern and dynamics: Water Resources Research, v. 41, p. 1 -9.

Davis, J.L., and Annan, A. P., 1989, Ground-penetrating radar for high-resolution mapping of soil and rock stratigraphy: Geophysical Prospecting, v. 37, p. 531-551.

Ferguson, R., and Ashworth, P., 1991, Slope-induced changes in channel character along a gravel-bed stream: the Allt Dubhaig, Scotland: Earth Surface Processes and Landforms, v. 16, p. 65-82.

Ghinassi, M., and Ielpi, A., 2018, Morphodynamics of Torridonian fluvial braid bars revealed by three-dimensional photogrammetry and outcrop sedimentology: Sedimentology, v. 65, p. 492-516.

Gran, K., and Paola, C., 2001, Riparian vegetation controls on braided stream dynamics: Water Resources Research, v. 37, p. 3275-3283.

Hein, F.J., and Walker, R.G., 1977, Bar evolution and development of stratification in the gravelly, braided, Kicking Horse River, British Columbia: Canadian Journal of Earth Sciences, v. 14, p. 562-570.

Hey, R.D., and Thorne, C.R., 1986, Stable channels with mobile gravel beds: Journal of Hydraulic Engineering, v. 112, p. 671-689.

Hickin, A.S., Kerr, B., Barchyn, T.E., and Paulen, R.C., 2009, Using GPR ground-penetrating radar and capacitively coupled resistivity to investigate 3-D fluvial

architecture and grain-size distribution of a gravel floodplain in Northeast British Columbia, Canada: Journal of Sedimentary Research, v. 79, p. 457-477.

Hickson, T.A., Sheets, B.A., Paola, C,. and Kelberer, M., 2005, Experimental test of tectonic controls on three-dimensional alluvial facies architecture: Journal of Sedimentary Research, v. 75, p. 710-722.

Horn, J.D., Joeckel, R.M., and Fielding, C.R., 2012a, Progressive abandonment and planform changes of the central Platte River in Nebraska, central USA, over historical timeframes: Geomorphology, v. 139-140, p. 372-383.

Horn, J.D., Fielding, C.R., and Joeckel, R.M., 2012b, Revision of Platte River facies model through observations of extant channels and barforms, and subsurface alluvial valley fills: Journal of Sedimentary Research, v. 82, p. 72-91.

Huber, E. and Huggenberger, P., 2015, Morphological perspective on the sedimentary characteristics of a coarse, braided reach: Tagliamento River (NE Italy): Geomorphology, v. 248, p. 111-124.

Huggenberger, P., 1993, Radar facies: recognition of facies patterns and heterogeneities within Pleistocene Rhine gravels, NE Switzerland, *in*: Best, J.L. and Bristow, C.S., eds., Braided Rivers, Geological Society of London, Special Publication 75, p. 163-176.

Huggenberger, P., and Regli C., 2006, *in*: Sambrook Smith, G.H., Best, J.L., Bristow, C.S., and Petts, G.E., eds., Braided Rivers: Process, Deposits, Ecology and Management, International Association of Sedimentologists, Special Publication 36, p. 51-74.

Huisink, M., De Morre, J.J.W., Kasse, C., and Virtanen, T., 2002, Factors influencing periglacial fluvialmorphology in the northern European Russian tundra and taiga: Earth Surface Processes and Landforms, v. 27, p. 1223-1235.

Ielpi, A., 2017, Controls on sinuosity in the sparsely vegetated Fossálar River, southern Iceland: Geomorphology, v. 286, p. 93-109.

Ielpi, A. and Rainbird, R.H., 2015, Architecture and morphodynamics of a 1.6 Ga fluvial sandstone: Ellice Formation of Elu Basin, Arctic Canada: Sedimentology, v. 62, p. 1950-1977.

Ielpi, A., and Ghinassi, M., 2015, Planview style and palaeodrainage of Torridonian channel belts: Applecross Formation, Stoer Peninsula, Scotland: Sedimentary Geology, v. 325, p. 1-16.

Ielpi, A., and Rainbird, R.H., 2016, Reappraisal of Precambrian sheet-braided rivers: evidence for 1.9 Ga deep-channelled drainage: Sedimentology, v. 63, p. 1550-1581.

Jablonski, B.V.J., 2012, Process sedimentology and three-dimensional facies architecture of a fluvially dominated, tidally influenced point bar: Middle McMurray Formation, Lower Steepbank River Area, Northeastern Alberta, Canada, [Master's Thesis]: Queen's University, Kingston, Ontario, 371 p.

Jol, H.M., and Bristow, C.S., 2003, GPR in sediments: advice on data collection, basic processing and interpretation, a good practice guide, *in* Bristow, C.S., and Jol, H.M., eds., Ground Penetrating Radar in Sediments: Geological Society of London, Special Publication 211, p. 9-27.

Jones, C.M., 1977, Effects of varying discharge regimes on bed-form sedimentary structures in modern rivers: Geology, v. 5, p. 567-570.

Jones, L.S., and Schumm, S.A., 1999, Causes of avulsion: an overview, *in* Smith, N.D., and Rogers, J., eds., Fluvial Sedimentology VI, International Association of Sedimentologists, Special Publication 28, p. 171-178.

Lazarus, E.D., and Constantine, J.A., 2013, Generic theory for channel sinuosity: Proceedings of the National Academy of Sciences, v. 100, p. 8447-8452.

Leclerc, R.F., and, Hickin, E.J., 1997, The internal structure of scrolled floodplain deposits based on ground-penetrating radar, North Thompson River, British Columbia: Geomorphology, v. 21, p. 17-38.

Leclair, S.F., and Bridge, J.S., 2001, Quantitative interpretation of sedimentary structures formed by river dunes: Journal of Sedimentary Research, v. 71, p. 713-716.

Lunt, I.A., and Bridge, J.S., 2004, Evolution and deposits of a gravelly braid bar, Sagavanirktok River, Alaska: Sedimentology, v. 51, p. 415-432.

Lunt, I.A., Bridge, J.S., and Tye, R.S., 2004a, Development of a 3-D depositional model of braided-river gravels and sands to improve aquifer characterization, SEPM, Special Publication 80, p. 139-169.

Lunt, I.A., Bridge, J.S., and Tye, R.S., 2004b, A quantitative, three-dimensional depositional model of gravelly braided rivers: Sedimentology, v. 51, p. 377-414.

Miall, A.D., 1977a, A review of the braided-river depositional environment: Earth Science Reviews, v. 13, p. 1-62.

Miall, A.D., 1977b, Fluvial sedimentology: an historical review, *in*: Miall, A.D., eds., Fluvial Sedimentology, The Canadian Society of Petroleum Geologists, Memoir 5, p. 1-47.

Miall, A.D., 1983, Basin analysis of fluvial sediments, *in*: Collinson, J.D. and Lewin, J., eds., Modern and Ancient Fluvial Systems, International Association of Sedimentologists, Special Publication 6, p. 279-286.

Miall, A.D., 1985, Architectural-element analysis: a new method of facies analysis applied to fluvial deposits: Earth Science Reviews, v. 22, p. 261-308.

Miall, A.D., 1996, The geology of fluvial deposits: sedimentary facies, basin analysis, and petroleum geology: Berlin, Germany, Springer-Verlag Inc., 582 p.

Millar, R.G., 2000, Influence of bank vegetation on alluvial channel patterns: Water Resources Research, v. 36, p. 1109-1118.

Mumpy, A.J., Jol, H.M., Kean, W.F. and Isbell, J.L., 2007, Architecture and sedimentology of an active braid bar in the Wisconsin River based on 3-D ground penetrating radar, *in*: Baker, G.S.and Jol, H.M., eds., Stratigraphic Analyses using GPR, Geological Society of America, Special Paper 432, p. 111-131.

Murray, A.B., and Paola, C., 2003, Modelling the effect in vegetation on channel pattern in bedload rivers: Earth Surface Processes and Landforms, v. 28, p. 131-143.

Okazaki, H., Kwak, Y. and Tamura, T., 2015, Depositional and erosional architectures of gravelly braid bar formed by a flood in the Abe River, central Japan, inferred from a three-dimensional ground-penetrating radar analysis: Sedimentary Geology, v. 324, p. 32-46.

Parker, N.O., Sambrook Smith, G.H., Ashworth, P.J., Best, J.L., Lane, S.N., Lunt, I.A., Simpson, C.J. and Thomas, R.E., 2013, Quantification of the relation between surface morphodynamics and subsurface sedimentological product in sandy braided rivers: Sedimentology, v. 60, p. 820-839.

Reesink, A.J.H., Ashworth, P.J., Sambrook Smith, G.H., Best, J.L., Parsons, D.R., Amsler, M.L., Hardy, R.J., Lane, S.N., Nicholas, A.P., Orfeo, O., Sandbach, S.D., Simpson, C.J. and Szupiany, R.N., 2014, Scales and causes of heterogeneity in bars in a large multi-channel river: Rio Parana, Argentina: Sedimentology, v. 61, p. 1055-1085.

Rice, S.P., Church, M., Wooldridge, C.L., and Hickin, E.J., 2009, Morphology and evolution of bars in a wandering gravel-bed river; lower Fraser River, British Columbia, Canada: Sedimentology, v. 56, p. 709-736.

Rust, B.R., 1972, Structure and process in a braided river: Sedimentology, v. 18, p. 221-245.

Rust, B.R., 1977, Depositional models for braided alluvium, *in*: Miall, A.D., eds., Fluvial Sedimentology, The Canadian Society of Petroleum Geologists, Memoir 5, p. 85-88.

Sambrook Smith, G.H., Ashworth, P.J., Best, J.L., Woodwards, J., and Simpson, C.J., 2005, The morphology and facies of sandy braided rivers: some considerations of scale invariance, *in* Blum, M.D., Marriott, S.B. and Leclair, S.F., eds., Fluvial Sedimentology VII, International Association of Sedimentologists, Special Publication 35, p. 145-158.

Sambrook Smith, G.H., Ashworth, P.J., Best, J.L., Woodward, J. and Simpson, C.J., 2006a, The sedimentology and alluvial architecture of the sandy braided South Saskatchewan River, Canada: Sedimentology, v. 53, p. 413-434.

Sambrook Smith, G.H., Best. J.L., Bristow, C.S., and Petts, G., 2006b, Braided rivers: where have we come in 10 years? Progress and future needs, *in*: Sambrook Smith, G.H., Best, J.L., Bristow, C.S., and Petts, G.E., eds., Braided Rivers: Process, Deposits, Ecology and Management, International Association of Sedimentologists, Special Publication 36, p. 1-10.

Sambrook Smith, G.H., Ashworth, P.J., Best, J.L., Lunt, I. A., Orfeo, O. and Parsons, D.R., 2009, The sedimentology and alluvial architecture of a large braid bar, Rio Parana, Argentina: Journal of Sedimentary Research, v. 79, p. 629-642.

Sambrook Smith, G.H., Best, J.L., Ashworth, P.J., Lane, S.N., Parker, N.O., Lunt, I.A., Thomas, R.E. and Simspon, C. J., 2010, Can we distinguish flood frequency and magnitude in the sedimentological record of rivers?: Geology, v. 38, p. 579-582.

Schumm, S.A., 1968, Speculations concerning paleohydrologic controls of terrestrial sedimentation: Geological Society of America, Bulletin, v. 79, p. 1573-1588.

Schumm, S.A., 1985, Patterns of alluvial rivers: Annual Review of Earth and Planetary Sciences, v. 13, p. 5 -27.

Skelly, R. L., Bristow, C.S. and Ethridge, F.G., 2003, Architecture of channel-belt deposits in an aggrading shallow sandbed braided river: the lower Niobrara River, northeast Nebraska: Sedimentary Geology, v. 158, p. 249-270.

Smith, N.D., 1970, The braided stream depositional environment: Comparison of the Platte River with some Silurian clastic rocks, North-Central Appalachians: Geological Society of America, Bulletin, v. 81, p. 2993-3014.

Smith, N.D., 1974, Sedimentology and bar formation in the Upper Kicking Horse River, a braided outwash stream: The Journal of Geology, v. 82, p. 205-223.

Smith. D.G., 1976, Effect of vegetation on lateral migration of anastomosed channels of a glacier meltwater river Geological Society of America, Bulletin, v. 87, p. 857-860.

Tal, M., and Paola, C., 2007, Dynamic single-thread channels maintained by the interaction of flow and vegetation: Geology, v. 35, p. 347-350.

Tal, M. and Paola, C., 2010, Effects of vegetation on channel morphodynamics: results and insights from laboratory experiments: Earth Surface Processes and Landforms, v. 35, p. 1014-1028.

Thorne, C.R., Russell, A.P.G. and Alam, M.K., 1993, Planform pattern and channel evolution of the Brahmaputra River, Bangladesh *in*: Best, J.L. and Bristow, C.S., eds., Braided Rivers, Geological Society of London, Special Publication 75, p. 257-276.

Walker, R.G., 1976, Facies models 3: Sandy fluvial systems: Geoscience Canada, v. 3, p. 101-109.

Welber, M., Bertoldi, W. and Tubino, M., 2012, The response of braided planform configuration to flow variations, bed reworking and vegetation: the case of the Tagliamento River, Italy, in: Earth Surface Processes and Landforms, v. 37, p. 575-582.

Whiting, P.J., Dietrich, W.E., Leopold, L.B., Drake, T.G. and Shreve, R.L., 1988, Bedload sheets in heterogeneous sediment: Geology, v. 16, p. 105-108.

Williams, P.F. and Rust, B.R., 1969, The sedimentology of a braided river: Journal of Sedimentary Petrology, v. 39, p. 649-679.

Wooldridge, C.L. and Hickin, E.J., 2005, Radar architecture and evolution of channel bars in wandering gravel-bed rivers: Fraser and Squamish Rivers, British Columbia, Canada: Journal of Sedimentary Research, v. 75, p. 844-860.

2.11 Figures

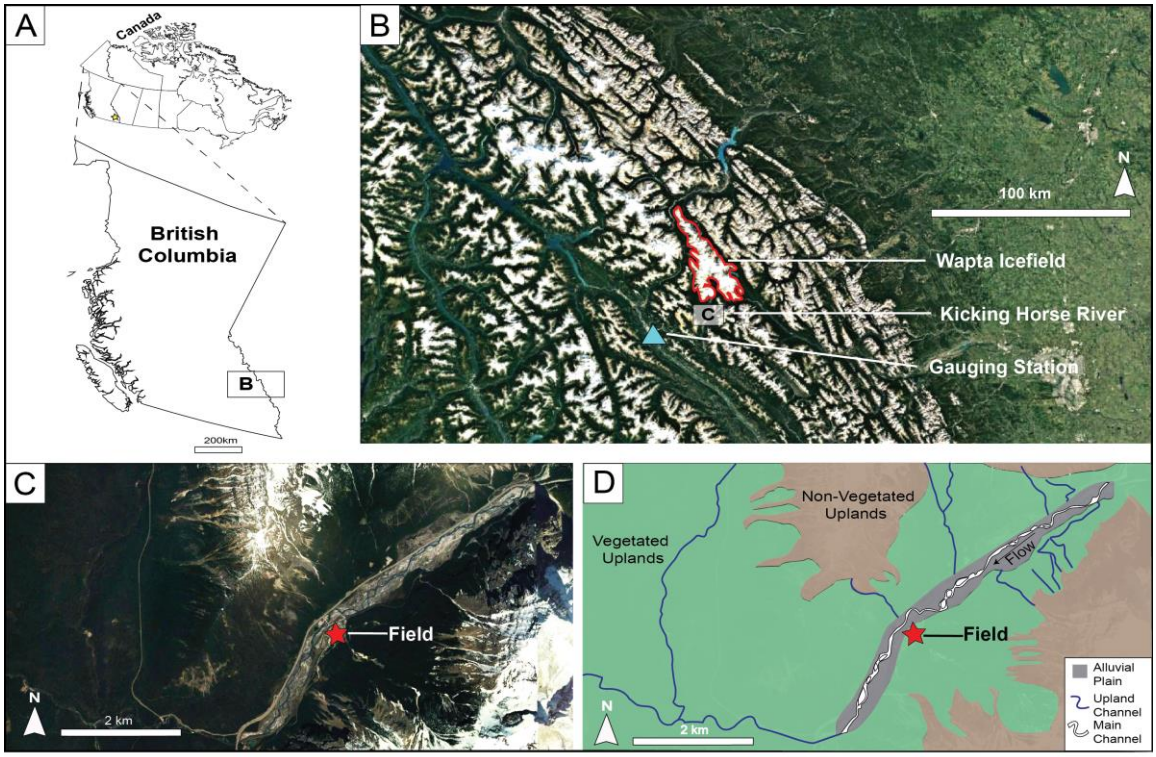

Figure 1: Regional setting

A) Location of study area in Field, British Columbia. **B)** Satellite inset showing source of the river (Wapta Icefield) and location of gauging station in Golden, BC. **C)** Satellite inset of 7 km alluvial plain of Kicking Horse River. **D)** Geomorphic map of study area.

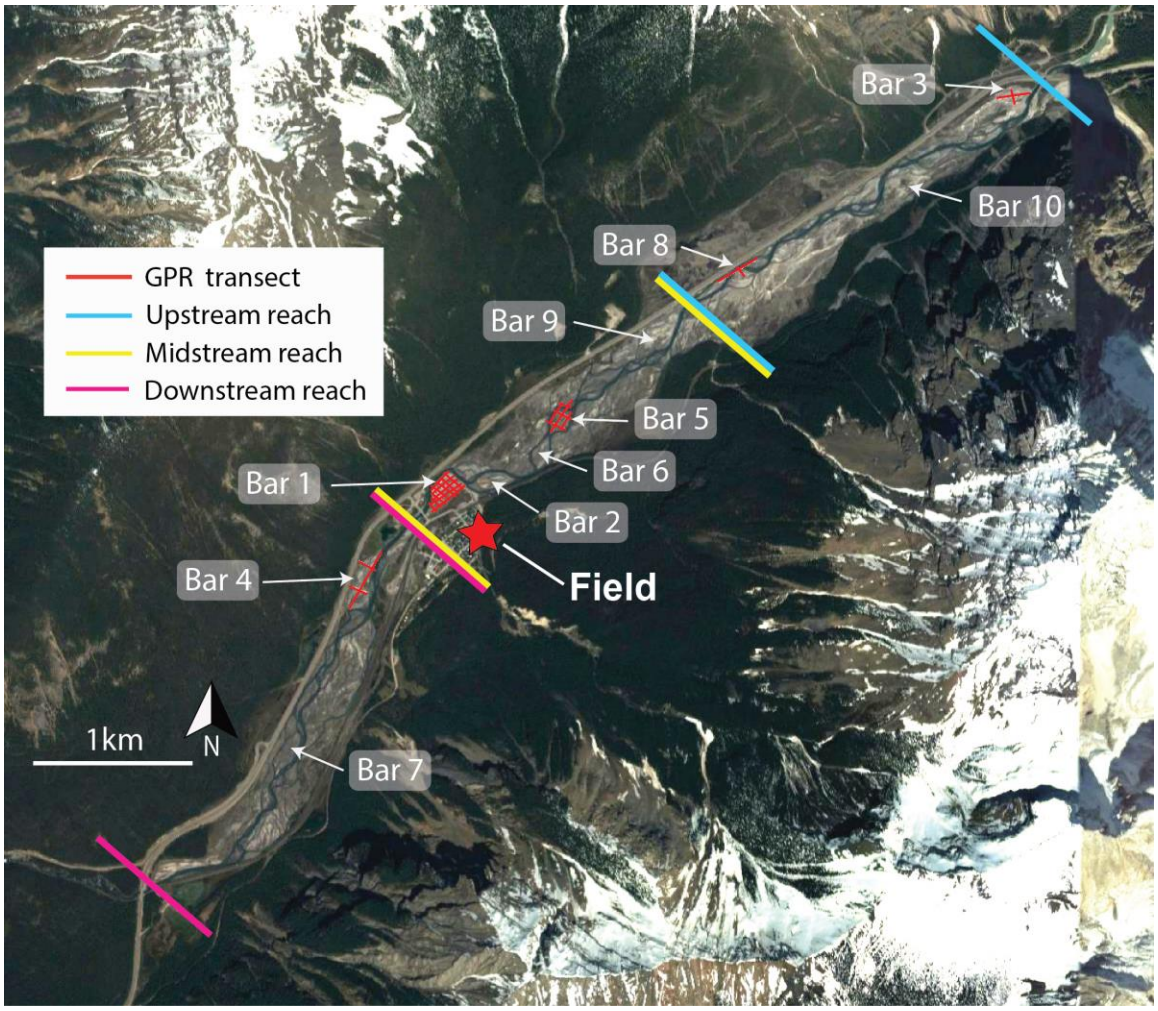

Figure 2: Study and sampling locations

Satellite image showing location of ten bars selected for sedimentological analysis, five of which were selected for GPR analysis (red lines indicate GPR transects). The extent of the upstream reach is delineated by blue lines; the midstream reach is delineated by

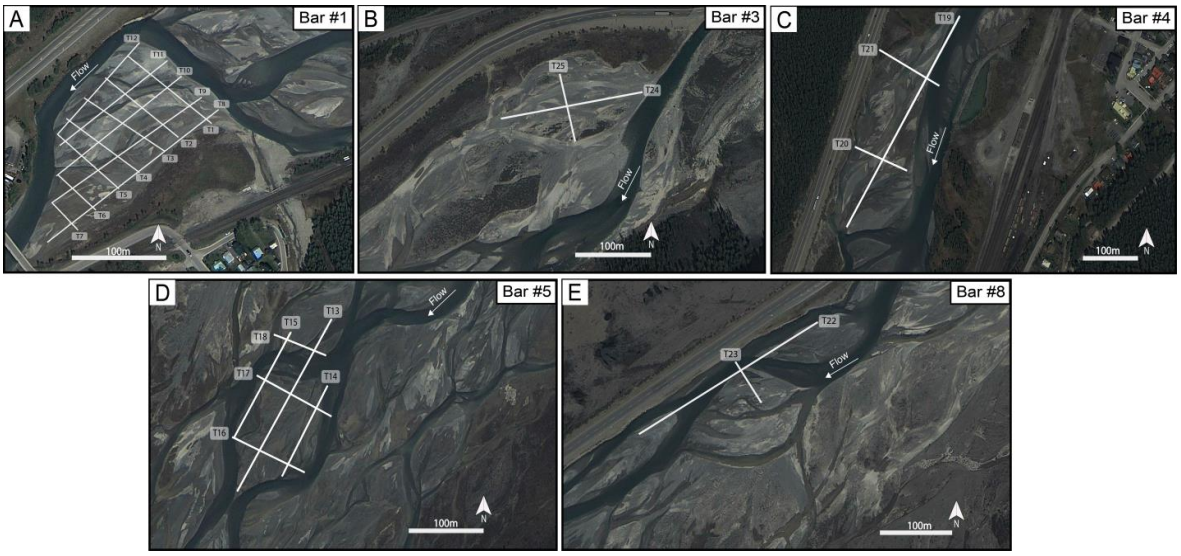

Figure 3: Ground-penetrating radar (GPR) survey locations

A) Bar #1, midstream reach, **B)** Bar #3, upstream reach, **C)** Bar #4, downstream reach, **D)** Bar #5, midstream reach, and **E)** Bar #8, upstream-midstream reach.

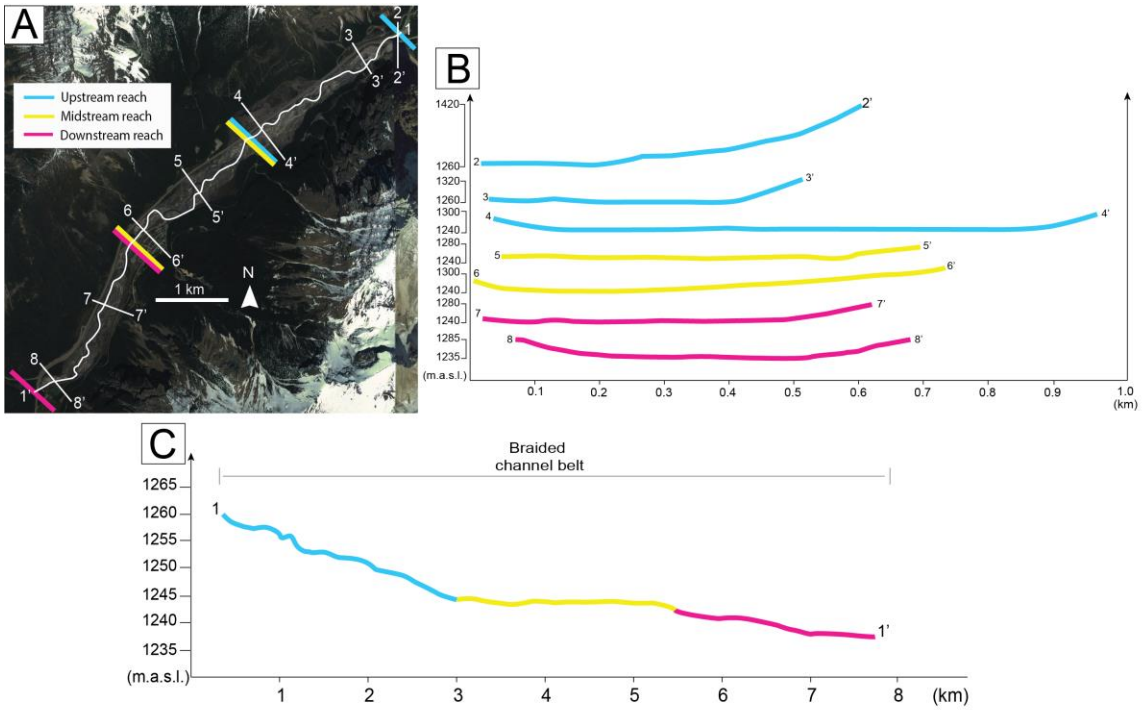

Figure 4: Topographic profiles of the study reach/valley bottom

A) Satellite image showing location of topographic profiles. **B)** Across-valley profiles showing width of valley. **C)** Down-valley profile of main braided channel. Upstream reach of alluvial plain delineated in blue; midstream reach delineated in yellow; downstream reach delineated in pink.

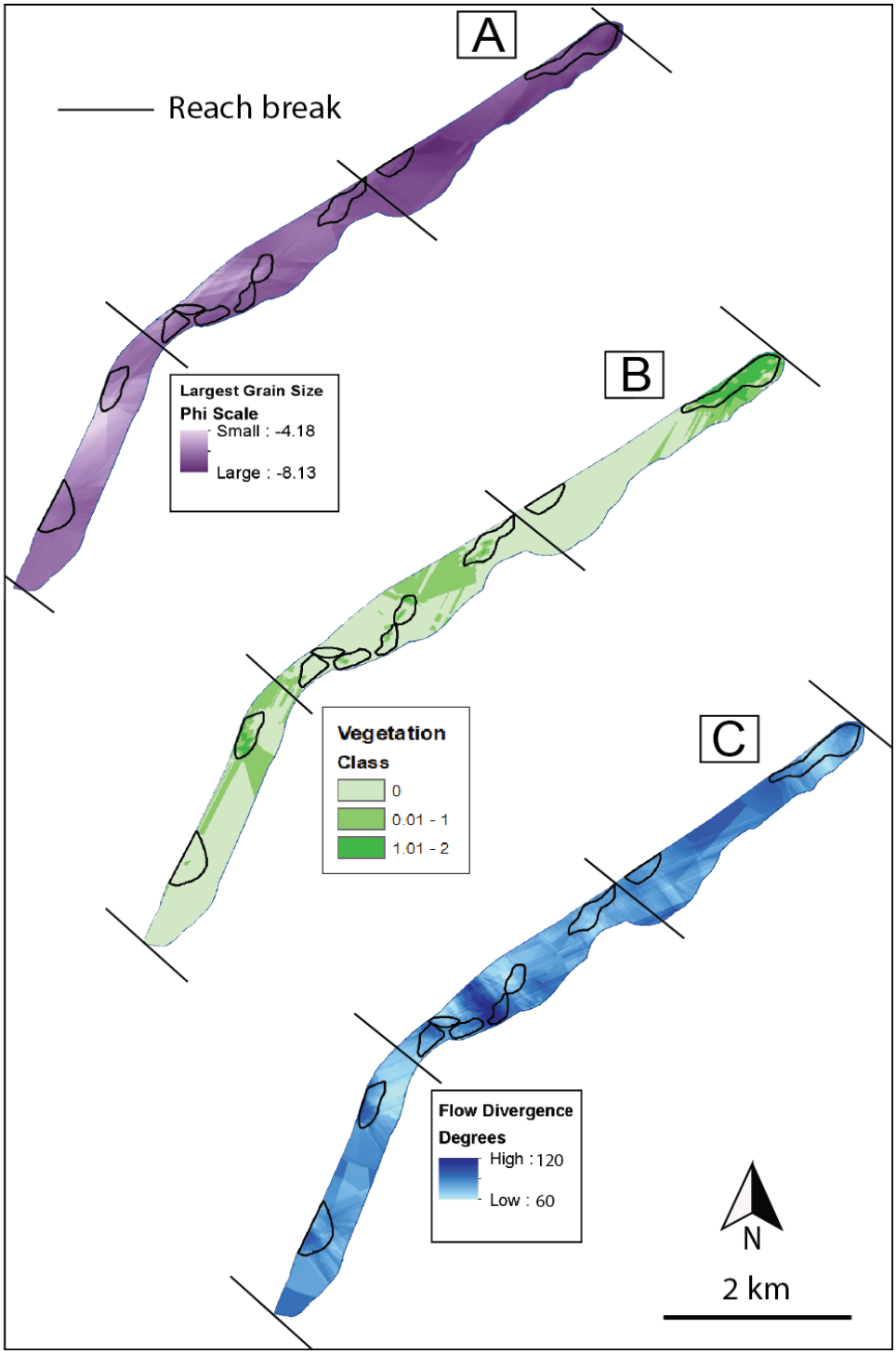

Figure 5: Kriging interpolation conducted in ArcMap on alluvial plain.

A) Largest grain size distribution (Phi scale). **B)** Vegetation cover on a scale of 0 to 4 (0 = No vegetation, 4 = Dense vegetation). **C)** Flow divergence values.

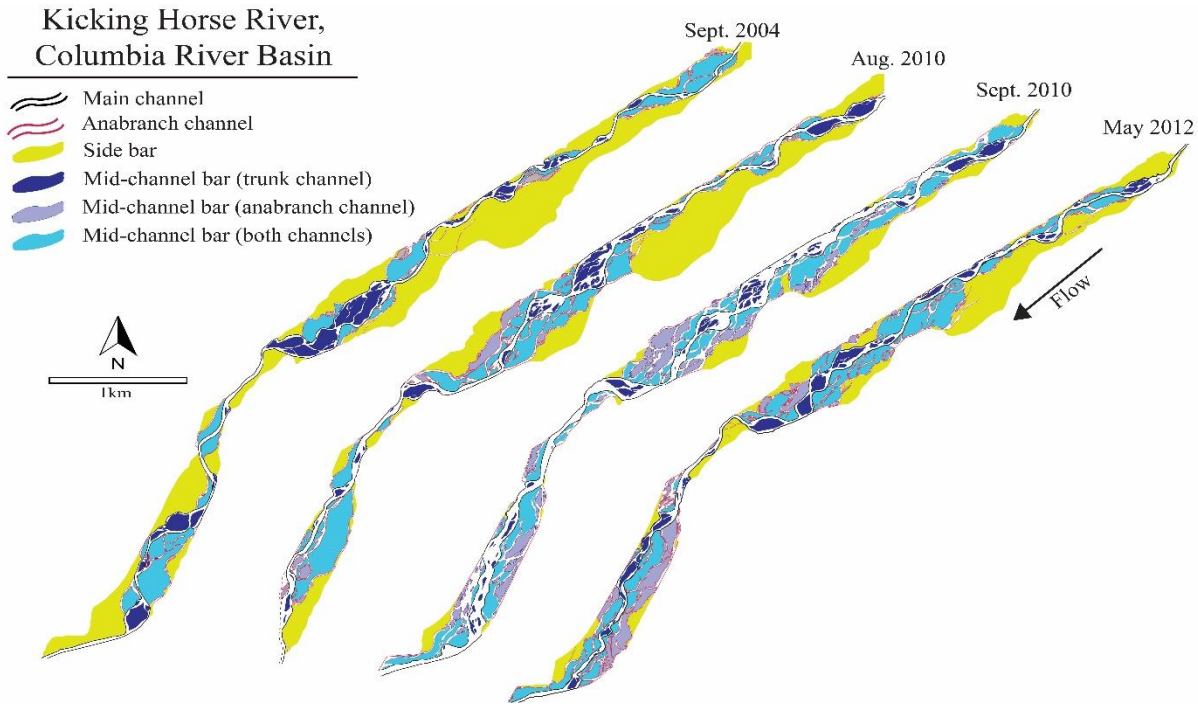

Figure 6: Remote sensing analysis

Map illustrating change in braided planform, generated from GeoEye-1™ satellite imagery. In September 2004 and August 2010, the river is at a low-flood stage. In September 2010 and May 2012, the river is at a high-flood stage.

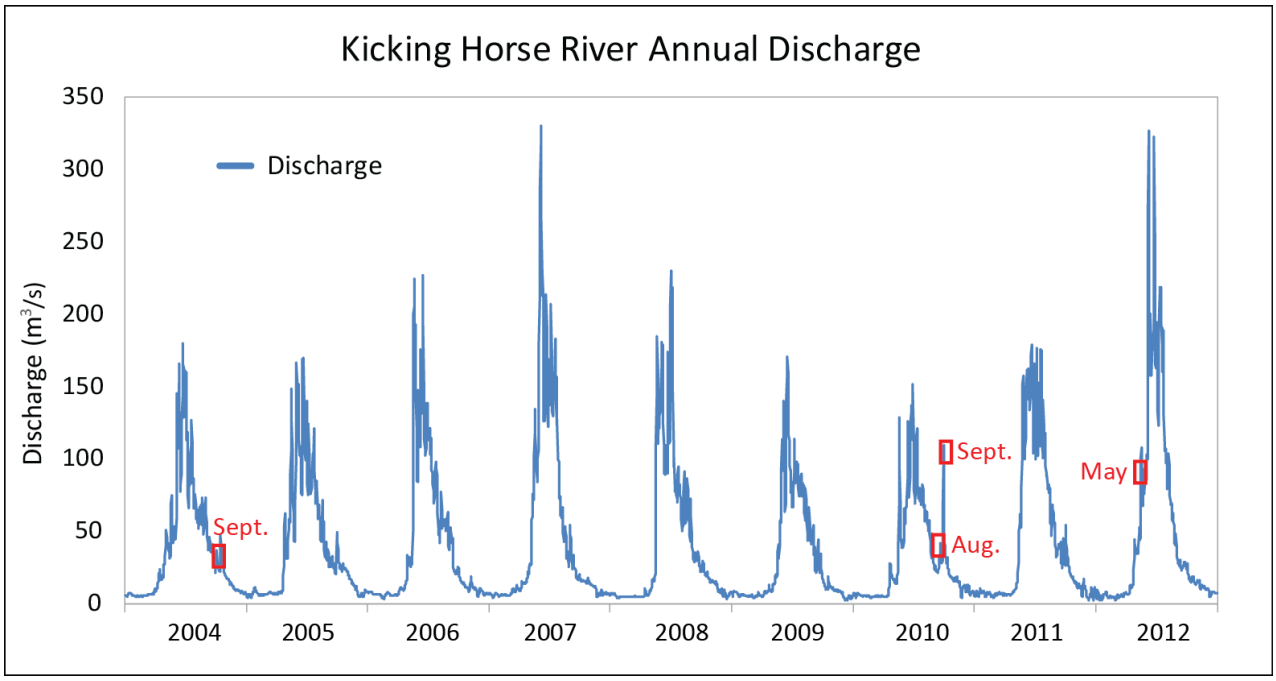

Figure 7: Stream flow hydrographs (2004-2012)

Annual discharge of the Kicking Horse River measured from gauging station 50 km downstream in Golden, BC.

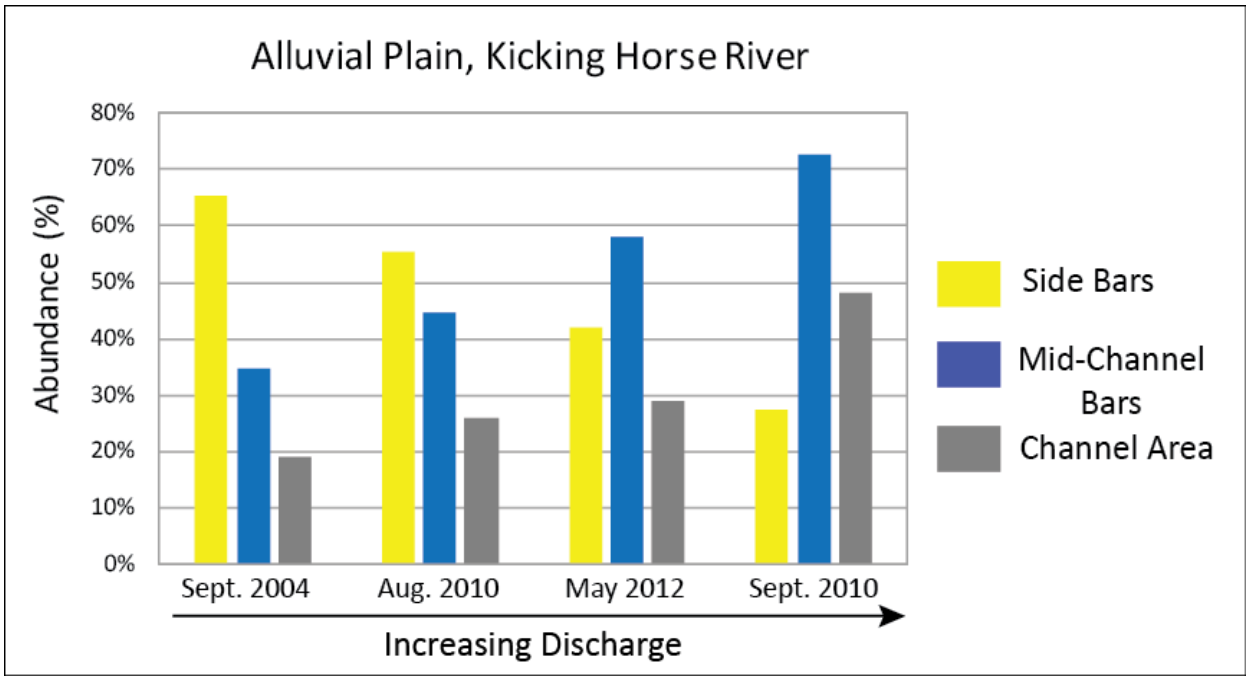

Figure 8: Bar and channel abundances

Comparison of the abundance of mid-channel bars to side bars with respect to varying discharge, derived from Geo Eye-1™ satellite imagery from September 2004 to May 2012, with the periods ordered by increasing discharge (m^3/s) to the right.

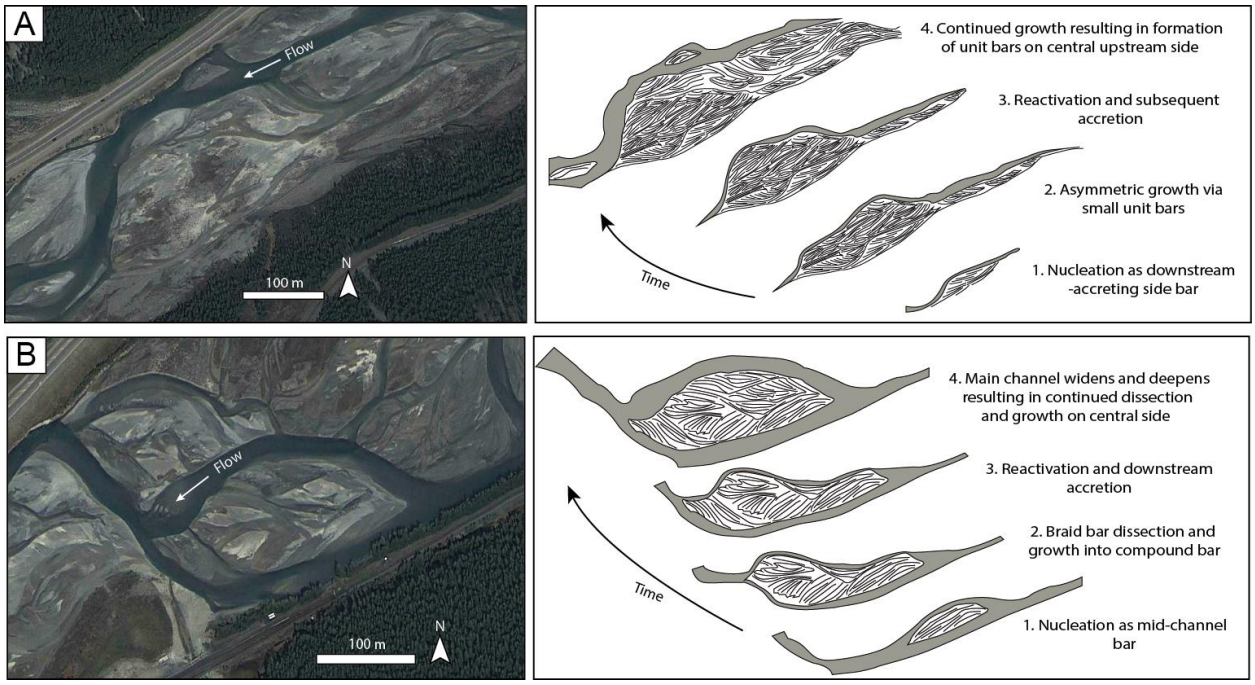

Figure 9: Morphological evolution of braid bars in the Kicking Horse River

A) Asymmetric growth of a valley-confined side bar. Side bar nucleation begins as downstream-accreting side bar and grows asymmetrically through multiple stages of reactivation and accretion. **B)** Growth, dissection, and subsequent reactivation of a valley-confined mid-channel bar. Mid-channel bars form from braid bar dissection and grow as the main channel widens and deepens.

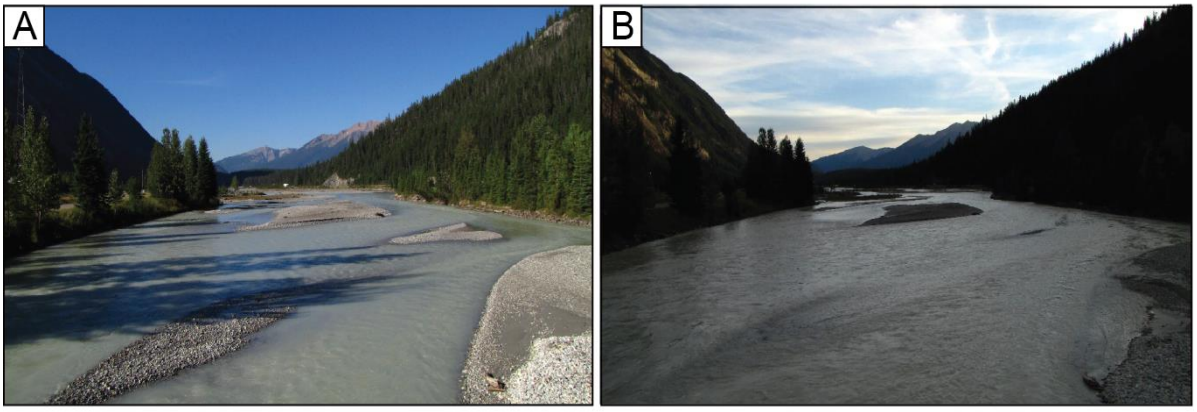

Figure 10: Photos of water level in midstream reach

A) Photo taken in A.M. on August 20, 2016, where mid-channel and side bars are well exposed. **B)** Photo taken same day in P.M. showing submersion of mid-channel bars and significant flooding of side bars.

Radar facies	*Description*	*Location*	*Depth of Occurrence*	*Interpretation*
1) Discontinuous 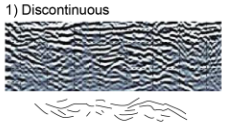	Discontinuous, undulatory reflectors that are not bound by any major or erosional surfaces; commonly trough-shaped and truncated; packages generally 2+ m thick and laterally continuous across GPR profiles	Variable; however higher occurrence in across-stream (transverse) transects	Variable	Crudely-stratified beds produced by small-dune migration, responsible for the construction of small-scale unit bars
2) Inclined 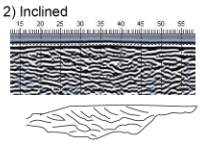	Sets of steeply dipping reflectors (10˚-20˚) in addition to low angle dipping reflectors (5˚-10˚); reflections commonly occur as lenses; packages are 50 cm - ~2 m thick (typically >1 m) and laterally continuous for 10-30 m	Higher occurrence in mid-stream and downstream regions of bars; high-angle reflectors occur close to bar margins	0-3 m	High amplitude and steeply dipping reflectors indicative of cross-stratification produced by avalanching fronts; low angle dipping reflectors represent accretion surfaces produced from the migration of bars
3) Horizontal 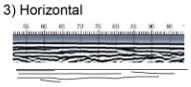	Horizontal to sub-horizontal, parallel to sub-parallel reflectors that are laterally continuous up to 120 m	Concentrated in upstream region of bars	0-2 m	Horizontally stratified beds indicative of bedload sheet migration and deposition on bar tops; smaller stratification related to lateral and vertical accretion of plane beds
4) Trough-Shaped 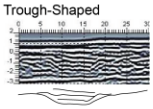	Small to large-scale concave-upwards reflectors typically bound by radar facies 2 and 3; laterally continuous for ~10-50 m	Variable	0-4 m	Small-scale to large-scale channel fill deposits that scale to flow depth; multi-storey channels (stacked channels) indicate multiple episodes of cut and fill at a variety of scales
5) Mounded 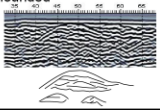	Isolated mound-shaped reflectors	Located throughout bar; however, solely observed in across-stream (transverse) transects	1-4 m	Mounds represent small scale unit bars or buried objects (logs, etc.)

Figure 11: Radar facies

Summary of radar facies 1-5 and their key characteristics and sedimentary interpretations.

See text for full facies descriptions.

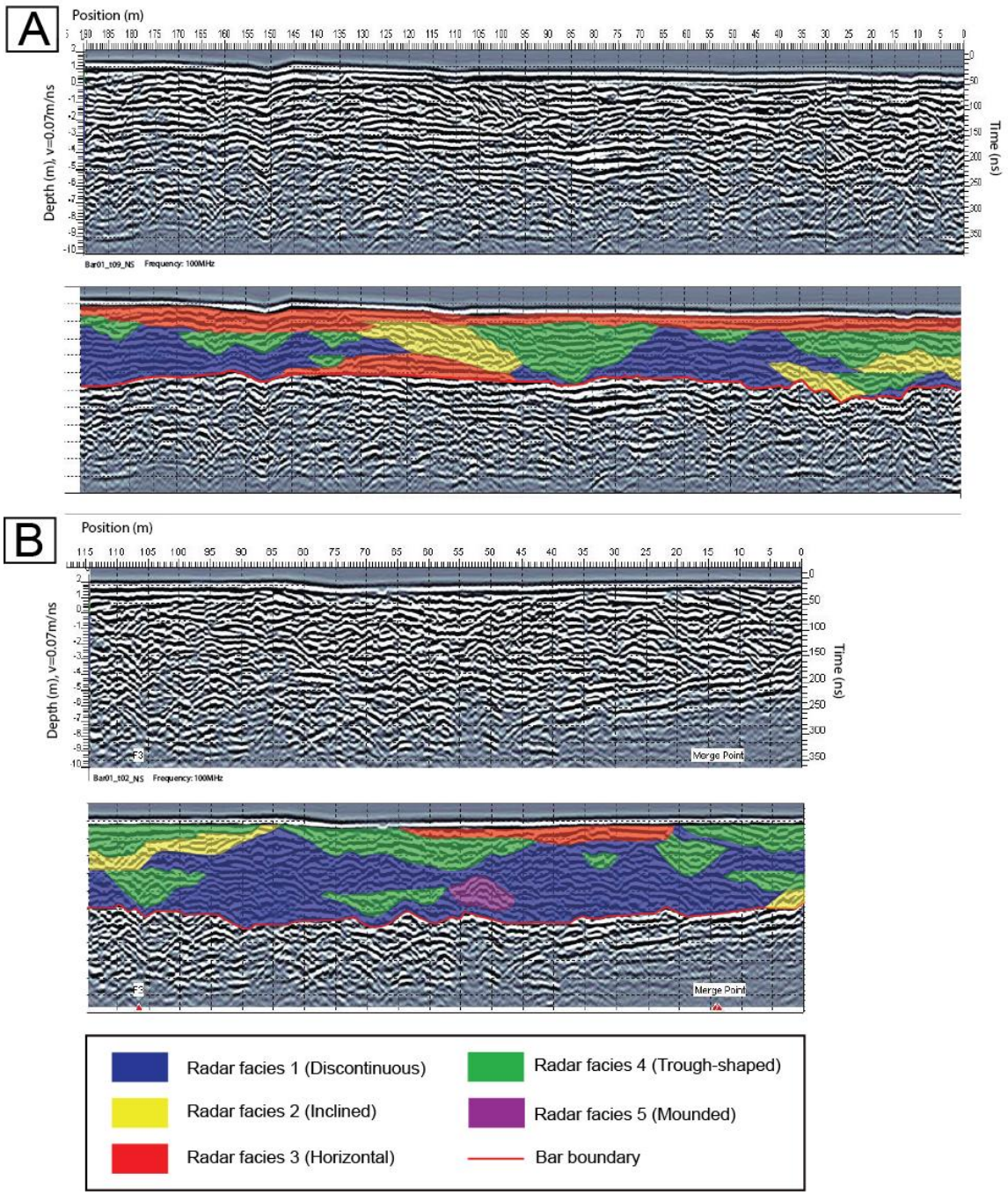

Figure 12: Examples of GPR data showing five primary radar facies

A) GPR data from downstream-oriented transect #9 in Bar 1. **B)** GPR data from across-valley transect #2 in Bar 1.

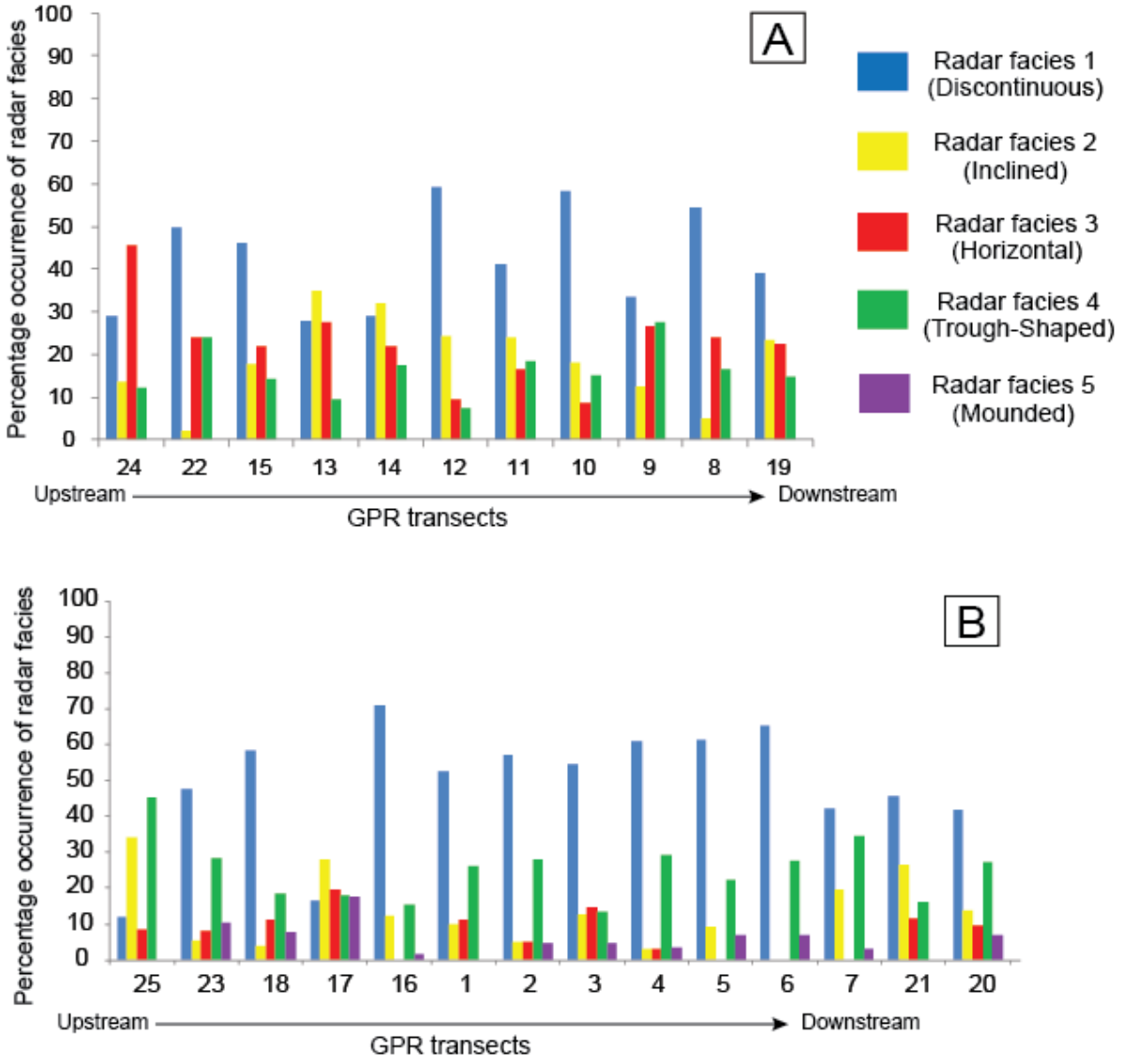

Figure 13: Percentage occurrence of radar facies

A) Downstream oriented GPR transects; and **B)** Across-stream oriented GPR transects. Transects are arranged from the most upstream transect (left-hand side) to the most downstream transect (right-hand side).

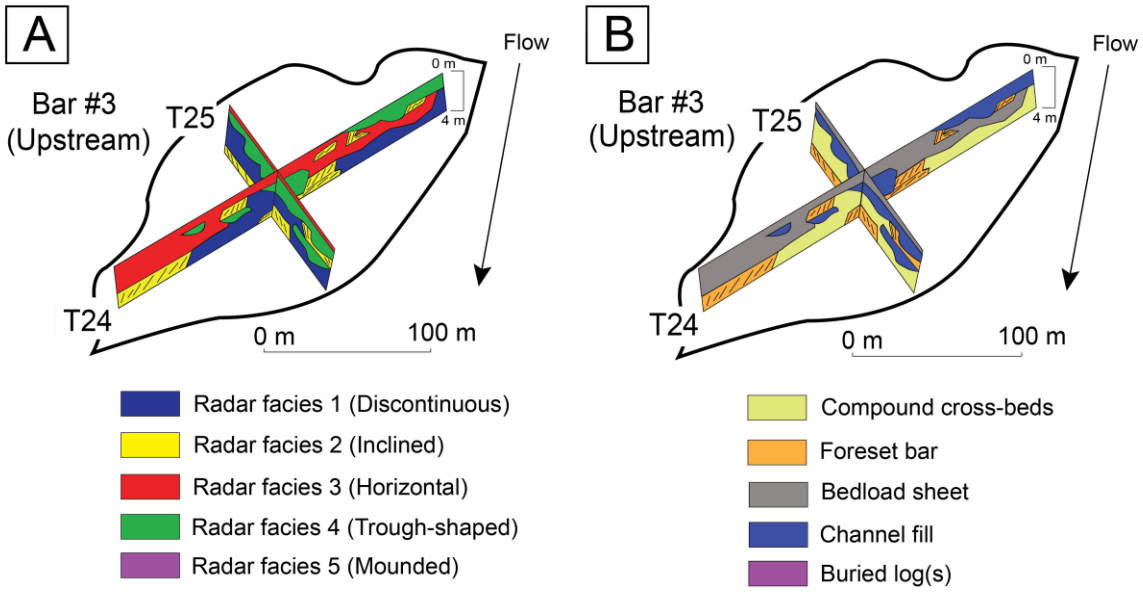

Figure 14: Three-dimensional GPR fence diagrams of Bar #3 (upstream)

A) Distribution of radar facies; and **B)** Distribution of interpreted preserved fluvial architectural elements.

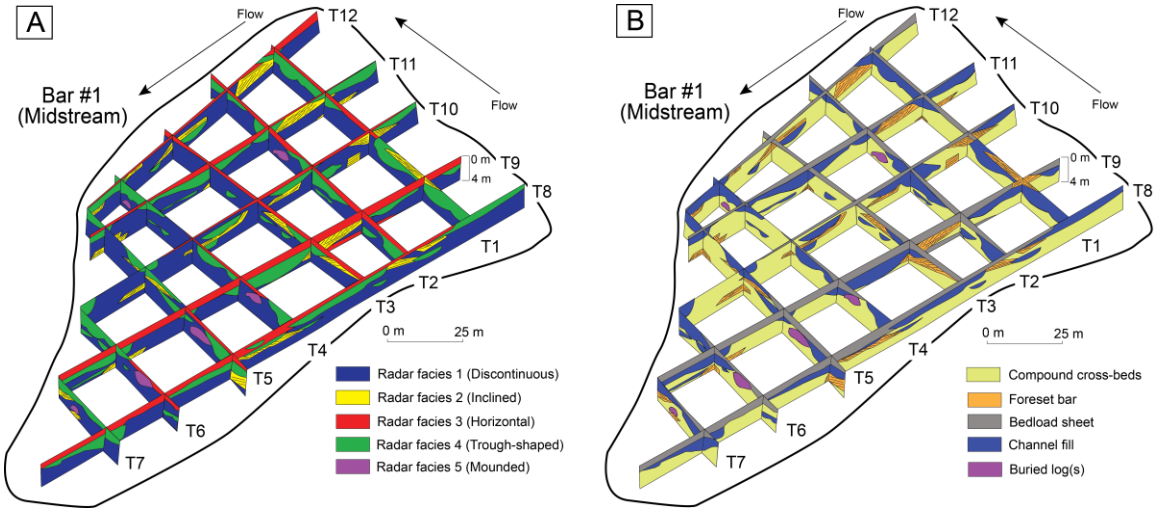

Figure 15: Three-dimensional GPR fence diagrams of Bar #1 (midstream)

A) Distribution of radar facies; and **B)** Distribution of interpreted preserved fluvial architectural elements.

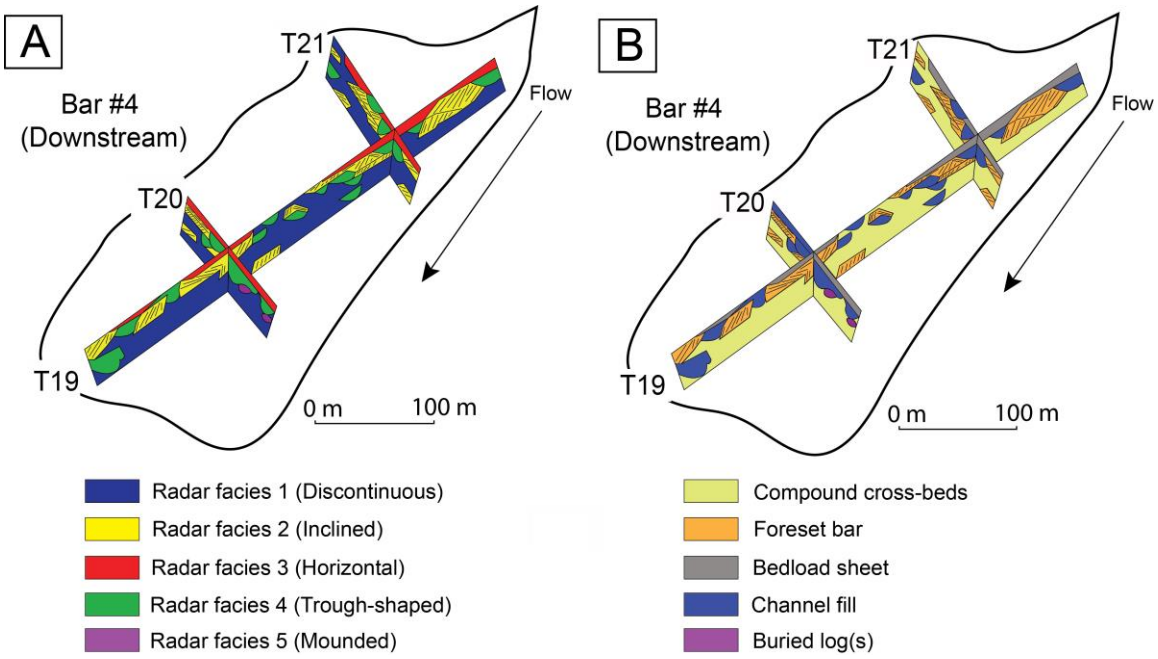

Figure 16: Three-dimensional GPR fence diagrams of Bar #4 (downstream)

A) Distribution of radar facies; and **B)** Distribution of interpreted preserved fluvial architectural elements.

Chapter 3

3. Concluding statements

3.1 Conclusions

This thesis investigated the sedimentology, discharge records, and subsurface alluvial architecture of the Kicking Horse River, a gravel-bed braided river located in southeastern British Columbia, Canada. Prior to this study, the sedimentology of the Kicking Horse River was last examined in the 1970's, and surprisingly the river still lacks a modern stratigraphic framework. This thesis re-examines the Kicking Horse River in terms of its sedimentology and integrates these observations with remote sensing over an eight-year period and ground-penetrating radar to develop a first integrated depositional model of the river. The study area encompasses a 7 km section of alluvial plain near the town of Field, British Columbia.

Ground observations and remote sensing highlight that the river's planform is dominated by large side bars formed from the amalgamation of unit bars at low-flow stages, and smaller, more abundant mid-channel bars prevalently developed at high-flood stage. Smaller anabranch channels are also prevalent when the river is at high flow with a larger discharge. Rates of lateral migration are as high as 9 m/year in the upstream reach, while in the downstream reaches of the river, lateral migration rates approach 34 m/year.

Five radar facies including discontinuous, horizontal, inclined, trough-shaped, and mounded reflections were identified. These facies were related to architectural elements

such as bedload sheets, channel fills, and unit bars preserved in the subsurface. Bedload sheets are the most abundant in the upstream reach where flow is confined to a single, deep channel. Unit bars are best preserved in the most downstream reach where the alluvial plain widens and becomes less confined. Channels fills are abundant throughout the alluvial plain, although a higher abundance of small channel fills was observed midstream where channel anabranching is prevalent.

Features described here bear many similarities to other modern and ancient fluvial systems. The upstream reach of the Kicking Horse River more closely resembles other gravel-bed braided systems, while the downstream reaches exhibit similarities to more sandy-gravel rivers that are braided to wandering in planform.

3.2 Future work

Chapter 2 concluded that the Kicking Horse River is dominated by architectural elements such as bedload sheets, channels, and bars (unit bars, mid-channel bars, and side bars). These elements are also observed in the subsurface alluvial architecture but are not as well preserved. This work however should be prompted with caution as models based on GPR only represent a small portion in time and cannot illustrate the entire morphodynamic evolution of an alluvial plain. Future work should focus on analyzing a higher number of bars and channel fills in the alluvial plain. Likewise, a historical analysis encompassing a larger amount of remote-sensing records would inevitably improve the accuracy of the proposed models.

4.4 Appendices

Appendix A: Ground-penetrating radar data for bar #1

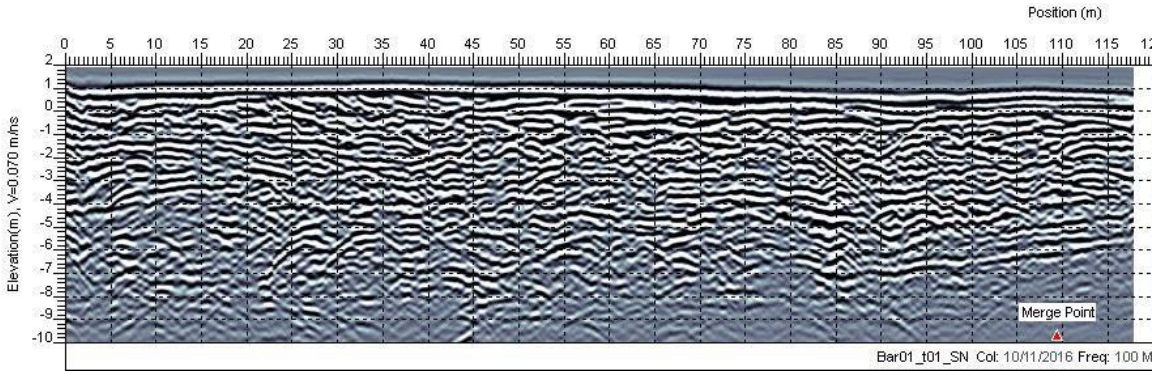

A1) GPR profile for bar #1, transect 1.

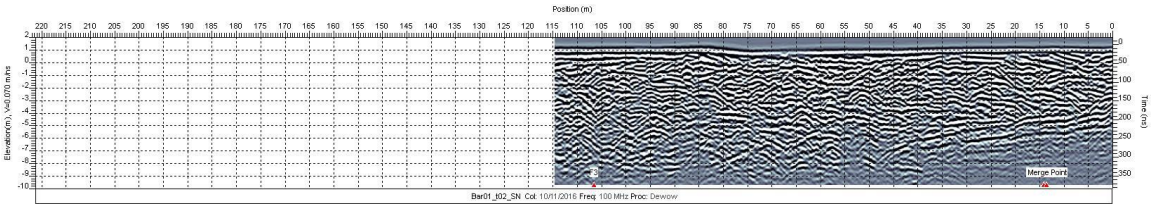

A2) GPR profile for bar #1, transect 2.

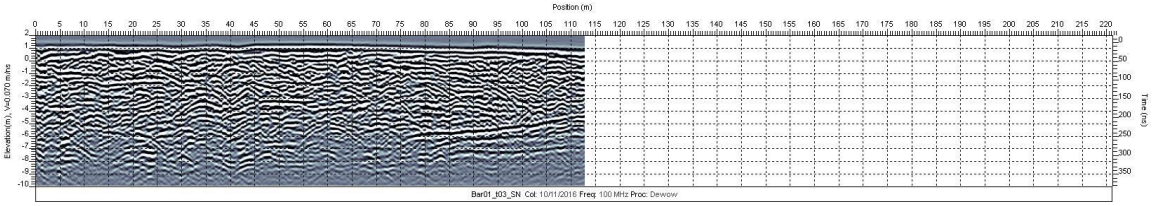

A3) GPR profile for bar #1, transect 3.

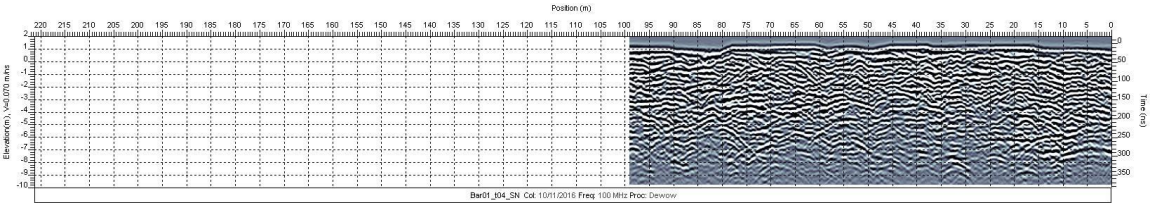

A4) GPR profile for bar #1, transect 4.

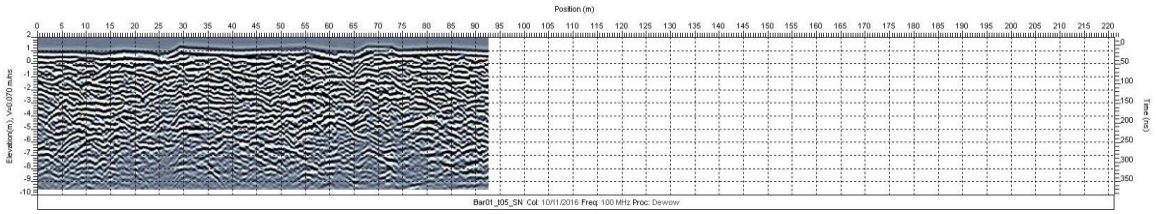

A5) GPR profile for bar #1, transect 5.

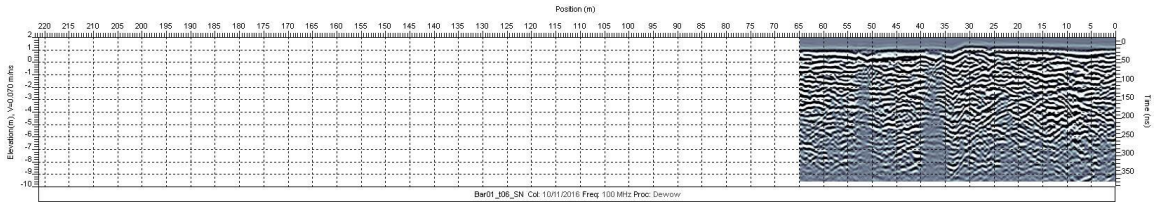

A6) GPR profile for bar #1, transect 6.

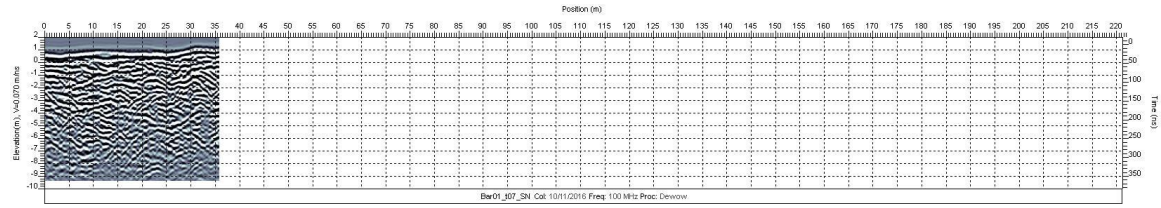

A7) GPR profile for bar #1, transect 7.

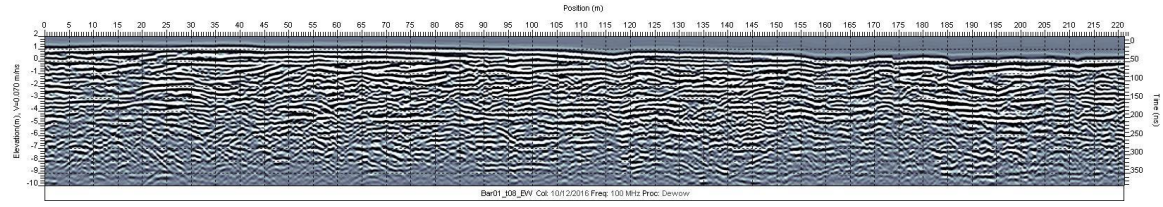

A8) GPR profile for bar #1, transect 8.

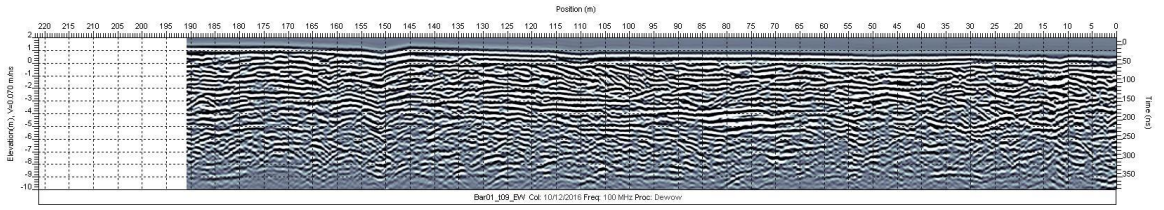

A9) GPR profile for bar #1, transect 9.

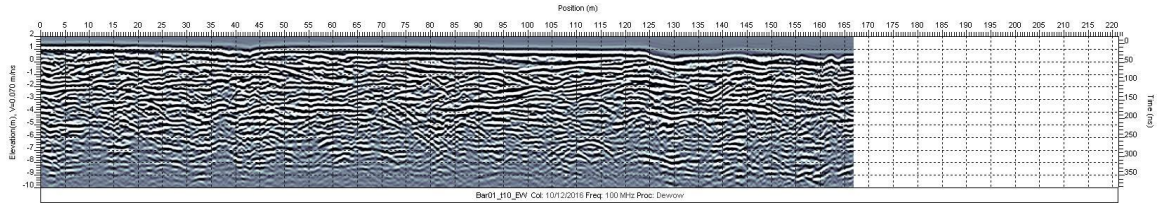

A10) GPR profile for bar #1, transect 10.

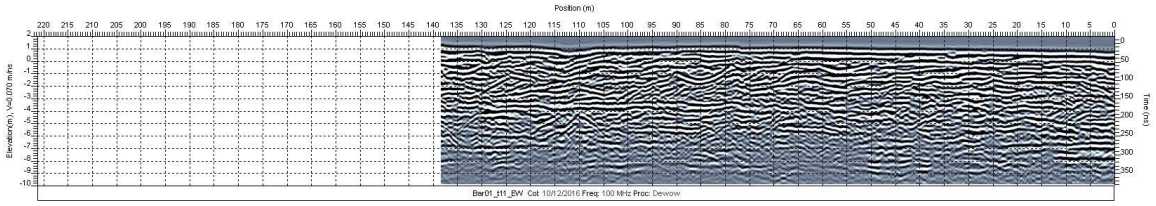

A11) GPR profile for bar #1, transect 11.

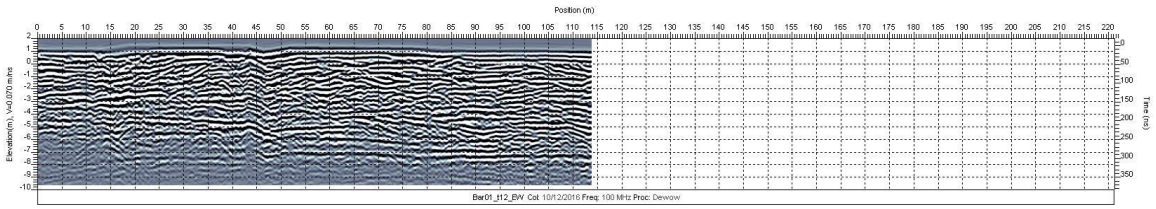

A12) GPR profile for bar #1, transect 12.

Appendix B: Ground-penetrating radar data for bar #3

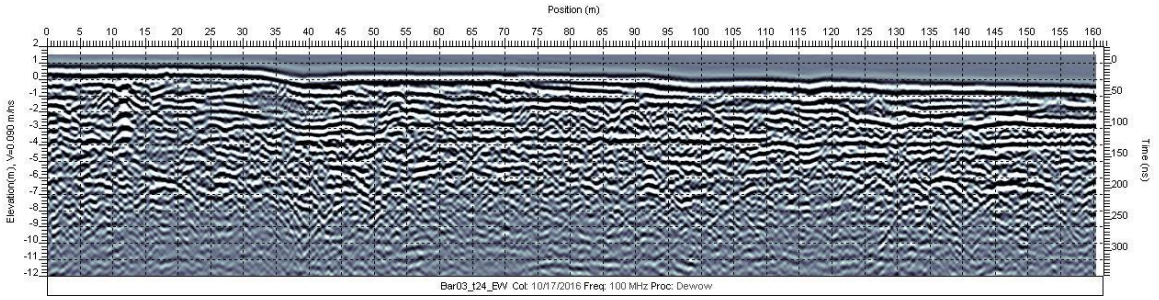

B1) GPR profile for bar #3, transect 24.

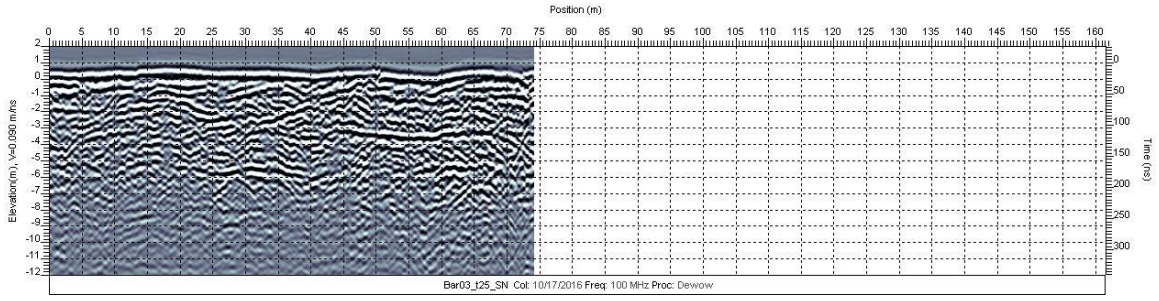

B2) GPR profile for bar #3, transect 25.

Appendix C: Ground-penetrating radar data for bar #4

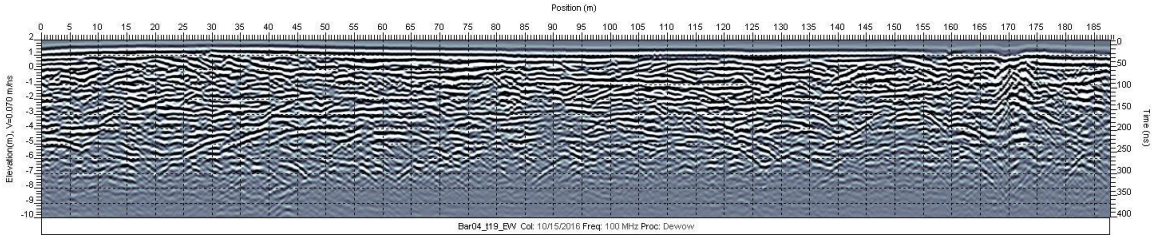

C1) GPR profile for bar #4, transect 19.

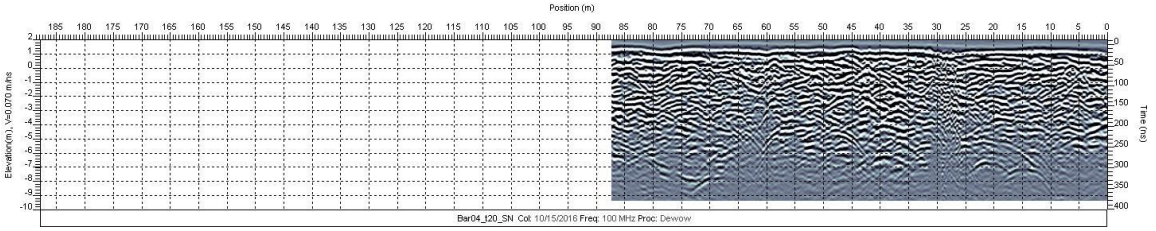

C2) GPR profile for bar #4, transect 20.

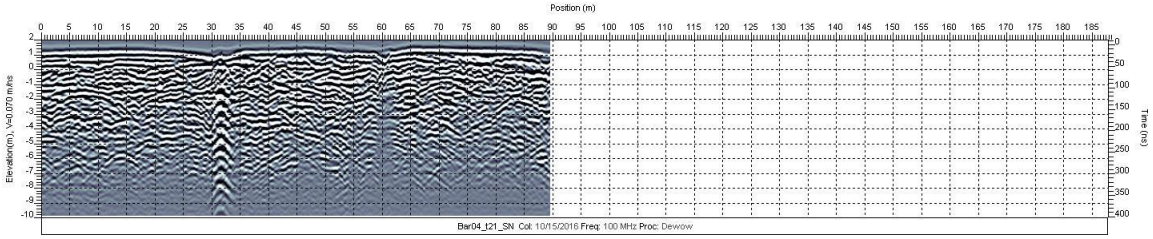

C3) GPR profile for bar #4, transect 21.

Appendix D: Ground-penetrating radar data for bar #5

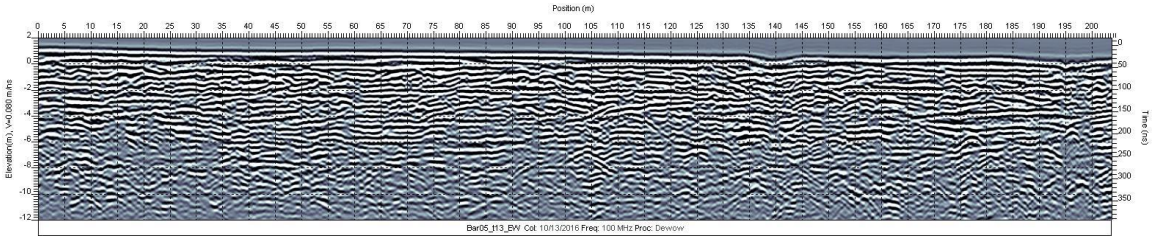

D1) GPR profile for bar #5, transect 13.

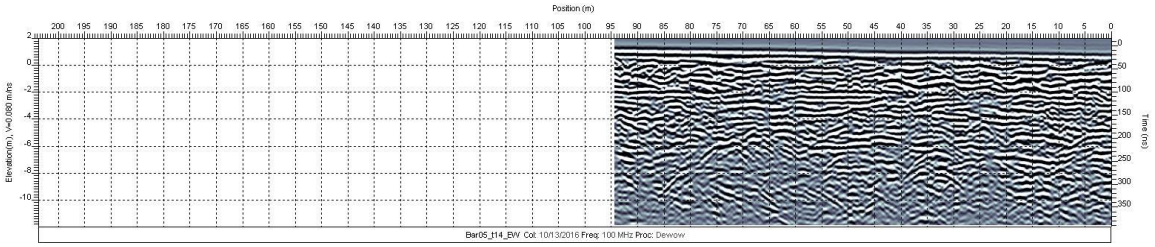

D2) GPR profile for bar #5, transect 14.

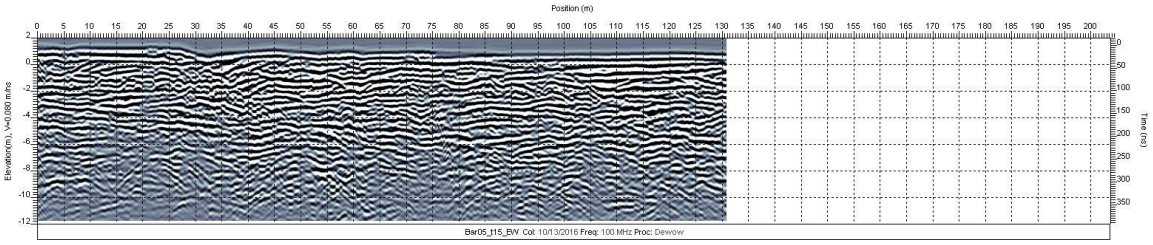

D3) GPR profile for bar #5, transect 15.

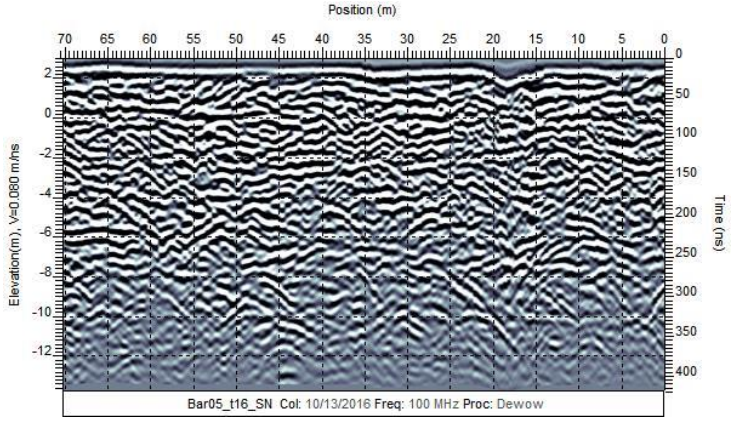

D4) GPR profile for bar #5, transect 16.

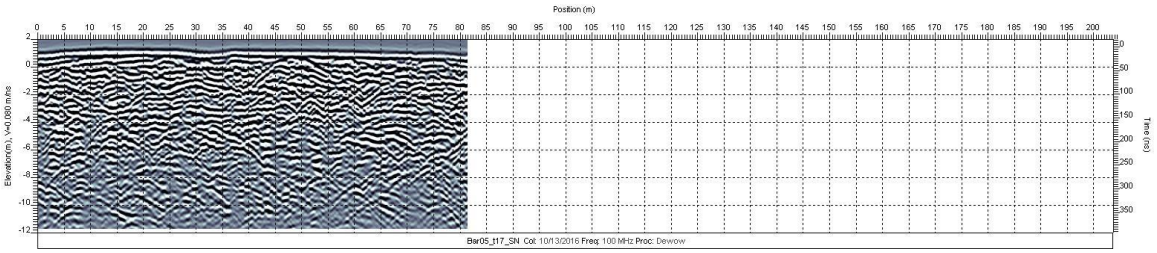

D5) GPR profile for bar #5, transect 17.

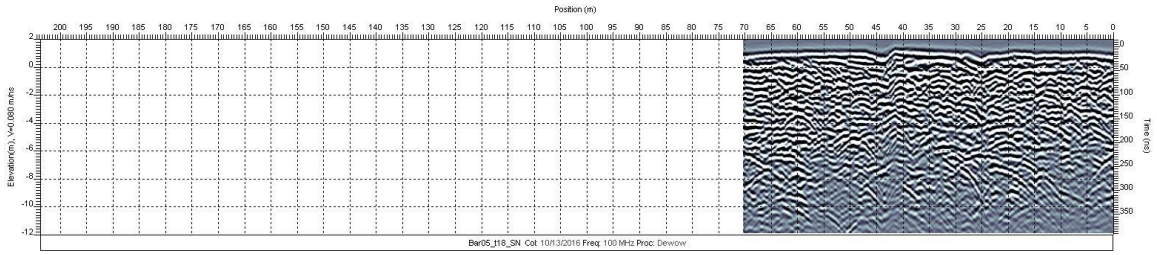

D6) GPR profile for bar #5, transect 18.

Appendix E: Ground-penetrating radar data for bar #8

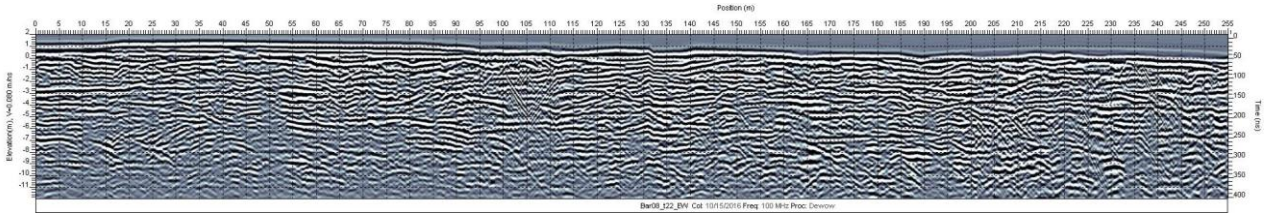

E1) GPR profile for bar #8, transect 22.

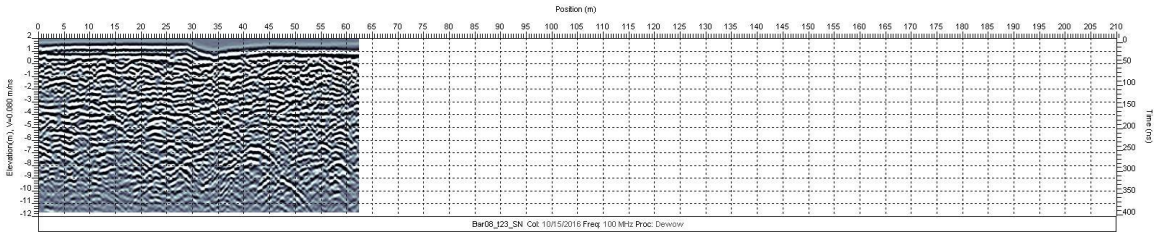

E2) GPR profile for bar #5, transect 23.